Elevated uranium concentration and low activity ratio (234U/238U) in the Œuf river as the result of groundwater–surface water interaction (Essonne river valley, South of Paris Basin, France)

Mathilde Zebracki, Christelle Marlin, Thierry Gaillard, Josselin Gorny, Olivier Diez, Valérie Monange, Véronique Durand, Charlotte Lafont, Cyrielle Jardin

▶ **To cite this version:**

Mathilde Zebracki, Christelle Marlin, Thierry Gaillard, Josselin Gorny, Olivier Diez, et al.. Elevated uranium concentration and low activity ratio (234U/238U) in the Œuf river as the result of groundwater–surface water interaction (Essonne river valley, South of Paris Basin, France). Science of the Total Environment, 2023, 876, pp.162537. 10.1016/j.scitotenv.2023.162537 . hal-04041118

HAL Id: hal-04041118
https://hal.science/hal-04041118

Submitted on 4 Apr 2023

HAL is a multi-disciplinary open access archive for the deposit and dissemination of scientific research documents, whether they are published or not. The documents may come from teaching and research institutions in France or abroad, or from public or private research centers.

L'archive ouverte pluridisciplinaire **HAL**, est destinée au dépôt et à la diffusion de documents scientifiques de niveau recherche, publiés ou non, émanant des établissements d'enseignement et de recherche français ou étrangers, des laboratoires publics ou privés.

Distributed under a Creative Commons Attribution - NonCommercial - NoDerivatives 4.0 International License

Title

Elevated uranium concentration and low activity ratio ($^{234}U/^{238}U$) in the Œuf river as the result of groundwater – surface water interaction (Essonne river valley, South of Paris Basin, France)

Author names and affiliations

Mathilde Zebracki*[1], Christelle Marlin[2], Thierry Gaillard[3], Josselin Gorny[1], Olivier Diez[1], Véronique Durand[2], Charlotte Lafont[1], Cyrielle Jardin[1], Valérie Monange[3]

[1]Institut de Radioprotection et de Sûreté Nucléaire (IRSN), PSE-ENV/SEDRE/LELI, 92260, Fontenay-aux-Roses, France

[2]Université Paris-Saclay, CNRS, GEOPS, 91405, Orsay, France

[3]Compagnie de Prospection Géophysique Française (CPGF)-HORIZON, 77210, Avon, France

*Corresponding author: mathilde.zebracki@irsn.fr

Keywords

Uranium, ($^{234}U/^{238}U$) activity ratio, river-groundwater interaction, selenium, Tertiary limestones, Beauce aquifer, Paris Basin, Essonne river

Abstract

Uranium (U) is a naturally occurring radioactive heavy metal widely distributed on Earth. Noticeable elevated U concentration and low activity ratio (AR) were occasionally detected in headwater stream of the Essonne river (Seine Basin, France), the namely Œuf river. This paper aims at providing new insight on geogenic U features in headwater streams and examines the role of river-groundwater interaction. The Œuf river was sampled four times in 2020 to investigate the influence of heterogenous geology and hydrological seasonality. The dissolved fraction of water samples was analyzed for a variety of chemical parameters (anion, major, minor and trace element concentrations, isotopes ^{234}U and ^{238}U). The Œuf river was shown to exhibit elevated U concentration up to 19.3 µg L^{-1} (exceeding by 100-fold the value of 0.19 µg L^{-1} known for riverine average) and low AR down to 0.41 (almost the third of the value expected in surface water, *i.e.*, 1.17). The Œuf river got enriched in U when receiving groundwater from Beauce Limestone Aquifer System. High U concentration (above 15 µg L^{-1}) was found in association with low AR (below 0.5) in the stream water when flowing in the outcrop zone of one BLAS unit. Taking advantage of changes in the stream flow conditions and the geochemical contrast between surface and ground waters, mixing volumes were calculated. This study first examined the potential of using U isotopes in combination with selenium as hydrogeochemical tracers of the river-groundwater continuum. In HWS, the aquifer discharge was shown to supply 12 to 59 % of the river water. This study demonstrates the key role played by the river-groundwater interaction on river water chemistry in small streams draining catchment with various geology setting. It also supports the use of combining redox sensitive trace elements to track the river-groundwater continuum.

Graphical abstract

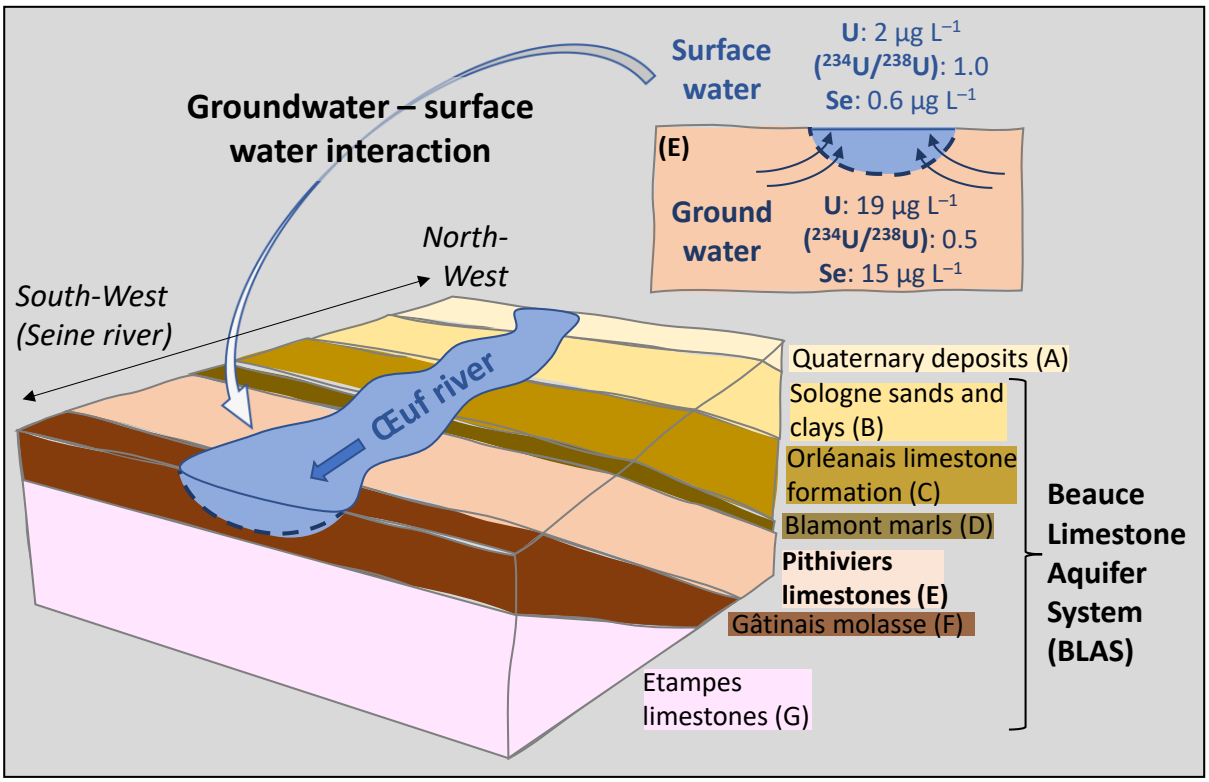

1 Introduction

Uranium (U) is a naturally occurring radioactive heavy metal that is widely distributed on Earth, *i.e.,* in rocks, sediments, soils and waters. In surface waters, U results from the weathering of soils and rocks and its concentration generally reflects the lithology of the weathered bedrock (F Chabaux, Riotte, & Dequincey, 2003; Ollivier, Radakovitch, & Hamelin, 2011; Zebracki et al., 2017). In worldwide riverine water (Palmer & Edmond, 1993), the average U concentration is assessed to be 0.19 µg L^{-1}. The concentration of U was initially examined in large rivers to quantify flux to ocean and it showed low fluctuations (Windom, Smith, Niencheski, & Alexander, 2000). Rivers draining small catchments are more likely to record larger variations of U concentration (Windom et al., 2000). Typically U concentration is reported below 4 µg L^{-1} in river water (Smedley & Kinniburgh, 2023). In certain basins (less than 1 %), streams show display natural elevated U concentration (Salminen et al., 2005) (above 10 µg L^{-1}), when draining specific areas containing U mineralization (Camacho et al., 2010; Salminen et al., 2005; Smedley & Kinniburgh, 2023; Snow & Spalding, 1994). Little is known about the geogenic fluctuations of U in small streams and increasing attention is given to U origin in agricultural draining areas (Gardner et al., 2022; Lyons, Gardner, Welch, & Israel, 2020). In groundwater, U concentration is reported to display much greater amplitude of variation with values ranging from 0.03 to 120 µg L^{-1} (Mangini, Sonntag, Bertsch, & Müller, 1979). The level of U concentration in groundwater is constrained by the oxidation-reduction potential, U being very soluble in oxidizing conditions and insoluble in reducing conditions. The alkaline character of the limestone formations favours U mobility in groundwater through the formation of stable U carbonate complexes (Banning, Demmel, Rüde, & Wrobel, 2013a). The weathering of geogenic source material and the desorption from mineral surfaces are the principal mechanisms of U release into groundwater (Riedel & Kübeck, 2018). Anthropogenic and geogenic causes might enhance U solubility in groundwater leading to the potential degradation of water drinking quality (Rosen, Burow, & Fram, 2019). Nitrate is a common contaminant deriving from surface-applied chemical fertilizer that fosters U mobility in groundwater (Nolan & Weber, 2015;

Riedel & Kübeck, 2018). In shallow aquifer, U mobility is favoured during the recharge of oxidizing water into the aquifer (Y. Wu, Wang, & Guo, 2019). Similarly, as U, selenium (Se) is trace element which mobility is also driven by redox conditions. The association of U and Se is typically found in U roll-front deposits (Bullock & Parnell, 2017; Howard III, 1977), which are produced by the groundwater transportation of dissolved elements from oxidized level to increasingly reduced and deep one. In sedimentary basin, deposits enriched in organic matter play an important role in U accumulation, in the forms of detrital material (Pregler et al., 2019), peat and lignite formations (Cumberland, Douglas, Grice, & Moreau, 2016; Pregler et al., 2019; Read et al., 1993). Argillaceous sediments enriched with organic matter and pyrite fulfilling karst cavities were shown to concentrate together U and Se (Bassil et al., 2016).

Uranium has three U isotopes which are commonly detected in rocks: ^{238}U (half-life: $4.47\ 10^9$ y), ^{235}U ($7.04\ 10^8$ y) and ^{234}U ($2.46\ 10^5$ y). Both ^{238}U and ^{235}U are primordial radionuclides present on Earth since its formation, while ^{234}U has a radiogenic origin, being produced through the radioactive disintegration of ^{238}U. This radiogenic fractionation yields to a preferential leaching of ^{234}U relative to ^{238}U during the rock chemical weathering (Fleischer, 1980; Kigoshi, 1971). Consequently, surface and ground waters generally display an enrichment of ^{234}U with respect to ^{238}U, with corresponding ($^{234}U/^{238}U$) activity ratio (AR) above 1. Waters depleted in ^{234}U indicate that the weathered solid surface is also depleted in ^{234}U (Israelson, Bjrck, Hawkesworth, & Possnert, 1997; Mathieu, Bernat, & Nahon, 1995; Riotte & Chabaux, 1999). In soil leachates, ^{234}U deficit indicates that surface or subsurface soil have already experienced ^{234}U loss by leaching, as this has been pointed out in soil of river (Riotte & Chabaux, 1999) and lake (Israelson et al., 1997) catchments. The riverine value of AR is averaged 1.17 (François Chabaux, Riotte, Clauer, & France-Lanord, 2001). On a worldwide scale, the observation of ^{234}U deficit regarding ^{238}U (AR below 1) in freshwater is scarcely documented: single example is given by the Strengbach watershed (France) where a slight ^{234}U deficit has been occasionally documented in a stream (Riotte & Chabaux, 1999) (minimum AR of 0.966) and a spring (Pierret, Stille, Prunier, Viville, & Chabaux, 2014) (AR of 0.819). Little is known about geogenic AR fluctuation in small streams. Groundwaters exhibit a larger range of AR variation than surface waters, AR values commonly ranging from 0.9 to 12 (Osmond & Cowart, 1976). Extreme low AR values nearby or below 0.5 were detected as single values in a variety of hydrogeological settings (Abdul-Hadi, Alhassanieh, & Ghafar, 2001; Chkir, Guendouz, Zouari, Hadj Ammar, & Moulla, 2009; El-Aassy et al., 2015; Grabowski & Bem, 2012; Kaufman, Rydell, & Osmond, 1969). This extreme deficit in ^{234}U (with respect to ^{238}U) was taken as an indicator of specific hydrogeological areas with high permeability, rapid groundwater circulation and intense dissolution (Kaufman et al., 1969). The fractionation between ^{238}U and ^{234}U is specific of U and unique among the other heavy metals (Michel, Kraemer, & DeWayne Cecil, 2009; Osmond, Cowart, & Ivanovich, 1983). Taking advantage from this, U isotopes were shown to be relevant isotopic tracers in hydrological studies (Osmond & Cowart, 1976; Osmond, Rydell, & Kaufman, 1968), especially in tracking the groundwater circulation (F. Chabaux, Bourdon, & Riotte, 2008; Osmond & Cowart, 1976; Osmond, Kaufman, & Cowart, 1974; Rovan et al., 2020). Based on U isotopes ability to distinguish different water sources, they were used in river catchments as tracers of the interactions between groundwater and surface waters (Huckle et al., 2016; Navarro-Martinez et al., 2017; Pierret et al., 2014; Ryu, Lee, Chang, & Cheong, 2009). Infrequently U isotopes were utilized to quantify the groundwater contribution to surface water in combination with other tracers, as strontium isotopes (Durand, Chabaux, Rihs, Duringer, & Elsass, 2005; Paces & Wurster, 2014; Riotte & Chabaux, 1999) and major elements (Navarro-Martínez, Sánchez-Martos, Salas García, & Gisbert Gallego, 2020).

At the head of the Essonne river valley (Seine Basin), in the namely Œuf river, a maximum U concentration of 22 µg L^{-1} (100-fold the average riverine concentration) was occasionally detected in the framework of radiological national survey. In parallel, isotopes analyses conducted in the stream

river revealed AR values below 0.5, indicating a large deficit in ^{234}U compared to ^{238}U. So far, such low AR (half that of 1.17) has not been described in other surface waters around the world. The ground catchment of the Œuf river is part of the Beauce Limestone Aquifer System (BLAS), one of the major French aquifers in the Paris Basin. In this reservoir, high level of Se concentration (above 10 µg L^{-1}) was occasionally found in groundwater for drinking water supply (Cary, Joulian, Battaglia-Brunet, & Decouchon, 2018). The presence of Se anomaly is of geogenic origin and was attributed to Ypresian lignite layer (Lower Eocene) which is known to concentrate Se in association with U (Chery & Rouelle-Castrec, 2004; Gaillard, 2017; Gaillard & Garnier-Séréno, 2017). The role of river-groundwater interaction was examined in this study to provide new insight on geogenic U characteristics in small streams and to improve the understanding of such atypical observations for freshwater. Here we presented the results of investigations on the interaction of the river with aquifer geology and the influence of hydrological seasonality. Prior to this work, no hydrogeochemical study was performed in streams of the Essonne river valley. This study also first examines the potential of using U isotopes in combination with Se as hydrogeochemical tracers of the river-groundwater continuum.

2 Regional settings

The Paris Basin refers to a large sedimentary basin covering almost the northern half of France (Figure 1), whose deposits extend from Permian and Triassic at the base to Tertiary to Quaternary at the surface. It is drained by several rivers, amongst which the Seine River, being interconnected with large sedimentary aquifers.

The Essonne river is one of the major tributaries of the Seine river and it derives from the confluence of the Œuf river and the Rimarde river (Figure 1). The Œuf river originates as a small stream from the Grand Vau pond in the Orléans Forest located approximately 100 km south of Paris. The Œuf river flows through a South-West to North-East axis with a length pathway of approximately 32 km. The Œuf river drains a surface catchment of 282 km^2 with elevations ranging from 129 to 88 m above the sea level (masl). The slope of the river is 1.3 ‰ in average.

The Œuf river displays a mean annual discharge of 0.5 $m^3 s^{-1}$ (water discharge measured over the 1970 – 2010 period at Bondaroy station (Figure 1) ; data available from http://hydro.eaufrance.fr/). This river yearly exhibits two contrasted hydrological seasons: the high water season (HWS) from January to May and the low water season (LWS) from June to December.

The local geological formations typically comprise lacustrine limestones interbedded with detrital sedimentary formation. The riverbed consists in Quaternary alluvium, mainly clayey, and mostly covering Early and Middle Miocene geological formations. At the downstream river extremity, Oligocene geological formation starts outcropping. In detail, the Œuf river crosses upstream to downstream the following geological formations (Gigot, 1984) (A to F; Figure 1):

- From 0 to 3 km, the river starts as connected ponds (Grand Vau then Petit Vau) lying on Quaternary deposits “A”, Sologne sands and clays “B” (Late Langhian to Early Pliocene), Orléanais marls and sands C1 (Burdigalian);
- From 3 to 9.5 km, the river flows on Orléanais marls and limestones “C2” (Burdigalian);
- From 9.5 to 10.9 km, the river flows on Blamont marls “D” (Aquitanian);
- From 10.9 to 23.1 km, the river flows on Pithiviers limestones “E” (Aquitanian);
- From 23.1 to 32 km, the river flows on Gâtinais molasse “F” (Aquitanian).

The Œuf river ends when meeting the Rimarde river and that coincides with the outcrop of Etampes limestones G (Rupelian). The two Orléanais formations C1 and C2 are considered as lateral variation of Orléanais limestone formation unit; on Figure 1 they were distinguished based on the difference

reported between their lithological facies. Except for the Langhian and Burdigalian sandy deposits, this sedimentary pile of Tertiary lacustrine calcareous formations dating from Rupelian (Early Oligocene) to Aquitanian (Early Miocene) forms the upper part of the Beauce Limestone Aquifer System (BLAS). The BLAS (*sensu stricto*), approximatively 75 m thick, comprises three main aquifer units, *i.e*., Orléanais limestones, Pithiviers limestones and Etampes flinty limestones, separated by two aquitards, *i.e.*, Blamont marls and Gâtinais molasse.

South of the Œuf river catchment and below the Orléans Forest, the BLAS is overlaid by Orléanais marls and sands and by Sologne sands and clays (Figure 1). The geological formation of Sologne sands and clays is permeable at its top (due to the presence of sands) and more impermeable at its bottom (presence of clayey deposits), making the Sologne sand an additional aquifer in the studied area. The sandy texture of Orléanais formation is separated from Sologne sands by a paleosol containing a peat layer (Gigot, 1984). The Sologne detrital formation is known to come from the erosion of granite mountains located further south (Massif Central) (Rasplus, 1982). Based on the borehole cutting description (https://infoterre.brgm.fr/), the limestones of the Orléanais and the Pithiviers formations have a mudstone texture with pseudobreccia horizons.

At a larger scale, the BLAS is the upper part of the regional Beauce aquifer that comprises a thicker sedimentary series deposited from Eocene to Miocene (Ypresian to Burdigalian) above the Late Cretaceous Chalk (Martin, Giot, & Le Nindre, 1999). The Beauce aquifer is a 230 m-thick multi-layered aquifer of regional extension of *ca*. 9 – 10,000 km^2 that makes it one of the largest aquifers in France (Martin et al., 1999).

The Œuf river originates in the most western part of the Orléans Forest. Northwest to the Orléans Forest the Beauce Plateau consists in recent (Quaternary) fertile silts that are used for intensive agriculture, particularly of wheat. The hydrographic network on the Beauce Plateau displays a low density and a low elongation index of watercourses which correspond to the river headwaters either flowing to the Seine river (to the north) or to the Loire river (to the south) (Larue & Étienne, 2014). On the Beauce Plateau, the low density hydrographic network coupled with a moderate soil coverage, the presence of chasms (in the Orléans Forest) and an important karstic network (Lorain, 1973) (North of Orléans Forest, Pithiviers and Etampes limestone formations) lead to an important and rapid water infiltration to the aquifer (Desprez, 1983).

3 Materials and methods

3.1 River water

3.1.1 Sampling and field measurement

Surface water samples were collected in the Œuf river stretches corresponding to the different formation outcrops and at the different hydrological seasons LWS and HWS. The Œuf river was sampled four times in 2020 in March (HWS), and in June, September, and December (LWS). To investigate the interaction between the Œuf river and the outcropping geological formations, twelve sampling sites were selected (R1 to R12, from B to F; Figure 1):

- R1 at 1.1 km and R2 at 1.6 km are in the outcrop zone of Sologne sands and clays followed by Orléanais marls and sands (B and C1, ending at 3 km),
- R3 at 4.9 km, R4 at 8.2 km and R5 at 9.2 km are in the outcrop zone of Orléanais marls and limestones (C2, from 3 to 9.5 km),
- R6 at 12.3 km, R7 at 14.1 km, R8 at 15.3 km, R9 at 16.3 km and R10 at 17.8 km are in the outcrop zone of Pithiviers limestones (E, from 10.9 to 23.1 km),
- R11 at 24.9 km and R12 at 29.5 km are in the outcrop zone of Gâtinais molasse (F, from 23.1 to 32 km).

The most upstream sampling site (R1) is in the Petit Vau pond which is hydraulically connected to the Grand Vau pond (main spring). The most downstream sampling site (R12) is 2.5 km before the Œuf – Rimarde confluence. Four tributaries (T1 to T4) meeting the Œuf river at 1.5, 8.6, 10.0 and 11.2 km respective distances from the spring were also sampled (Figure 1). During LWS, we noticed that the riverbed was dried out in the first 12.3 – 14.1 km of the Œuf river and in the four tributaries. On the contrary, we noticed that the spring area of the Œuf river (Grand Vau pond) was permanently filled.

Single samples of river water were collected considering the water mass was homogeneous owing to the stream small size (approximatively 2 m wide, 30 cm deep). In total, a set of 42 samples of river water was collected and stored in 50 mL-glass bottles and 1 L-polyethylene bottles in refrigerating conditions until they were transported to the laboratory (located approximately one hour's drive from the field, at Fontenay-aux-Roses, Paris south area), and prior to further treatment.
In parallel, physical and physico-chemical parameters were measured on field using a portable multi-parameter system (WTW Multi 3420) connected to single and specific probes for the determination of the temperature (T) and the electrical conductivity (EC; TetraCon 925), pH (SI Analytics ADA S7/IDS) and the oxidation-reduction potential (ORP; WTW Sentix). The ORP was measured with a reference electrode Ag/AgCl (3 M KCl), with a potential equal to 208 mV versus the Standard Hydrogen Electrode (SHE). All redox potential (Eh) values reported in the text are expressed versus the SHE electrode. For field measurement, the deviation was estimated at ± 10 % for each probe.

3.1.3 Sample preparation

The sample preparation was performed within 24 hours after sampling at IRSN laboratory LUTECE (Laboratoire Unifié d'expérimenTation Et de Caractérisation dans le domaine des dEchets). All water samples were filtrated (at 0.45 or 0.7 µm threshold) and the dissolved fraction was subsequently analyzed.

For carbon analysis, the water sampled with glass bottle was filtrated through glass fibre filter at 0.7 µm (Whatman). The dissolved fraction was then collected in 30 mL-glass bottle and immediately analyzed for carbon measurement.

For other chemical species, the water sampled with polyethylene bottle was filtrated through cellulose acetate membrane at 0.45 µm (Sartorius). The dissolved fraction was stored in 50 mL-polypropylene tube (VWR) then immediately analyzed for anion measurement; it was acidified with 0.3 M HNO_3 then stored at 4 °C prior to elemental analyses.

For U isotope analysis, the sample preparation procedure was completed by spiking each sample with a double isotope reference standard (Richter et al., 2008) (IRMM 3636) and followed by a separation step using UTEVA extraction chromatographic resin (Horwitz et al., 1992) (Eichrom Technologies). An aliquote of each filtered and acidified water sample (5 mL) to pH 1 was analyzed to determine the required volume of filtered water sample. Additional filtration was only performed for water samples having U concentration lower than 5 µg L^{-1}. The filtered water sample was then evaporated to dryness in 50 mL-polypropylene tube (VWR). The dry residue was dissolved in 4 mL 3 M HNO_3 and mixed with 10 µL of IRMM 3636 double spike with a $^{233}U/^{236}U$ isotope ratio of 1:1 and an initial ^{236}U concentration at 8.67 ng g^{-1}.

3.1.4 Chemical analyses

Only the dissolved fraction (< 0.45 µm) of the water samples was analyzed and all analyses were performed at IRSN laboratory LUTECE. Analytical settings are detailed in Supplementary information –

Materials and methods. For each measurement, the uncertainty derives from the standard analytical deviation and is given at ± 2 σ.

Concentration of anions SO_4^{2-}, NO^{3-}, Cl^-, F^-, Br^- and PO_4^{3-} was measured using ionic chromatography (Metrohm 930 Compact IC). Dissolved organic and inorganic carbon was measured using a carbon analyzer (Elementar TOC Vario). Concentration of the chemical elements Ca, Na, K, Si, Mg, Ba and Sr was determined using ICP-OES (Thermo Fisher Scientific iCAP 7600 Duo). The determination of U and Se concentrations and ($^{234}U/^{238}U$) activity ratio was performed using Agilent 8800 Inductively coupled plasma-Tandem mass spectrometry ICP-MS/MS (Agilent Technologies, Tokyo, Japan) equipped with an octupole collision/reaction cell (CRC) situated between two mass-selecting analysers.

3.2 Groundwater

Groundwater of BLAS units was not sampled through the study. We extracted data from the French national web portal ADES on groundwater (https://ades.eaufrance.fr/). Four boreholes (GW1 to GW4) were available in the vicinity of the Œuf river (Figure 1), and for each one, the drilling settings were examined: GW1 extracts groundwater from Orléanais limestone formation, GW2 and GW3 from Pithiviers limestones, and GW4 from both Pithiviers and Etampes limestones. A dataset of monitoring data acquired over the 2001 – 2021 timespan was compiled, including EC, ORP, the concentrations of Cl^-, NO_3^-, Ca, Mg, Se, U and the activities of isotopes ^{238}U and ^{234}U (allowing the computation of AR).

3.3 U speciation modelling

The choice of the thermodynamic database is known to impact the final speciation modelling of aqueous U in natural systems (Lartigue, Charrasse, Reile, & Descostes, 2020; Reiller & Descostes, 2020; X. Wang et al., 2019). In this study, we investigated the aqueous speciation of U in the presence of common inorganic ligands (Markich, 2002; Smedley, Smith, Abesser, & Lapworth, 2006), including OH^-, CO_3^{2-}, PO_4^{3-}, SO_4^{2-}, Cl^-, F^- and Br^-. The thermodynamic modelling code PHREEQC version 3 was used to compute U speciation (Parkhurst & Appelo, 2013), using the MINTEQ.V4 database (Eary & Jenne, 1992). The percentage of each U specie was based on its relative contribution to U concentration in water. The distribution of U aqueous species was calculated in the water samples displaying a complete chemical dataset only: R1 – R12 in March, R3 and R6 in June, R10 and R11 in September, and R1 – R3, R7, R8 and R10 – R12 in December.

4 Results

4.1 Stream water supply

Since we conducted a river survey at different times of 2020, we were able to observe differences in the river flow along the Œuf riverbed between LWS (March) and HWS (June, September and December).

In LWS, the water flow occurred permanently at R1 (1.1 km) which corresponds to the Grand Vau pond located nearby the spring of the Œuf river in the Orléans Forest. There, the geological formation of Sologne sands and clays is permeable at its top due to the presence of sands and more impermeable at its bottom due to the presence of clayey deposits. This is likely to explain the permanence of water at R1 that was attributed to the continuous discharge of Sologne sandy aquifer below the Orléans Forest. The Œuf riverbed was found occasionally dry in the outcrop zones of Orléanais formation (between R2 at 1.6 km to R5 at 9.2 km), indicating a loss of the stream water. Also, we noticed the absence of water in the four tributaries (T1 to T4) preventing from discharge into the main stream at 1.5, 8.6, 10.0 and 11.2 km. Permanent water flow was seen from 14.1 km (R7), indicating a water supply through groundwater discharge once the river flows over the Pithiviers limestones (10.9 – 23.1 km). The intermittent flow observed at the beginning of Pithiviers limestones (R6 at 12.3 km) indicates water table fluctuations with time. The zone where the stream flow became

continuous coincides with the disappearance of Blamont marls (aquitard) and the change of Pithiviers limestone aquifer from confined to unconfined (https://infoterre.brgm.fr/).

In HWS, the stream flow was permanent along the entire Œuf riverbed and its four tributaries, indicating that rainfall and its consecutive increasing water discharge is sufficient to maintain a continuous stream flow.

4.2 Stream water chemistry

The chemical results of the water sampled in the Œuf river catchment were reported in Tables 1 – 4 in Supplementary information. The spatial and seasonal variations of the stream water chemistry were illustrated on Figure 2 (physical and chemical parameters), Figure 3 (anion concentration) and Figure 4 (major, minor and trace element concentration).

Water ion balances were equilibrated for all sampling points with 10 % uncertainty. The Œuf river displayed pH values mostly comprised in the range 7 – 8, with lower values observed in LWS (7 – 7.5) compared to HWS (*ca*. 8). The pH of the stream water displayed circumneutral conditions, being in accordance with natural freshwater in carbonated environment. The ORP exhibited values mostly comprised in the range 330 – 550 mV, indicating the prevalence of oxidizing conditions being in accordance with water river conditions. Occasionally a low value (23 mV) was measured in December at 1.6 km when the stream water was shallow and stagnant.

Whatever the hydrological season (LWS or HWS), the dominant chemical species in the stream water were Ca (above 110 mg L^{-1} and 50 mg L^{-1} in LWS and HWS, respectively) and DIC (above 50 mg_C L^{-1} and 20 mg_C L^{-1} in LWS and HWS, respectively). Therefore, the stream water referred as calcium bicarbonate water, that being confirmed by the Piper diagram (Suppl. Inf. Figure 2). Concentration of NO_3^- was systematically above 30 mg L^{-1} in LWS, thus exceeding the European guideline alert value (*i.e.*, 25 mg L^{-1}; European Water Framework Directive 2000/60/EC).

Whatever the season, EC of the stream water globally increased downgradient, reflecting an increasingly degree of mineralization. The lowest values were seen at the most upstream site (R1 at 1.1 km), and the range of variation was narrow (39 – 51 µS cm^{-1}) whatever the hydrological season. The values increased up by a factor 20 downgradient, the highest values being found at the most downstream site (R12 at 29.3 km) where values varied almost 2-fold between LWS (898 µS cm^{-1} in September) and HWS (545 µS cm^{-1} in March).

Most chemical species and elements, including DIC (Figure 2), Cl^-, NO_3^-, SO_4^{2-}, F^-, Br^- (Figure 3), Ca, Mg, Na, K, Sr, and Se (Figure 4), generally exhibited concentration with a downgradient increase whatever the hydrological season (LWS or HWS). When comparing the concentrations between the hydrological season, the main contrast was their amplitude of variation: low concentrations were seen in HWS and high ones in LWS. Noticeably, Cl^-, Br^-, Na and K showed a sharp increase of concentration downstream in the outcrop zone of Gâtinais molasse. The variation of EC (Figure 2) was found to be in good agreement with the variations of DIC, Cl^-, NO_3^-, Mg, Ca, and Sr (correlation coefficients of 0.97, 0.91, 0.87, 0.96, 0.98 and 0.94, respectively; Suppl. Inf. Table 6).

The concentration of PO_4^{3-} varied by 2 orders of magnitude from 0.004 (R2) to 0.62 mg L^{-1} (R3). Also, it displayed differences between upstream and downstream, and between LWS and HWS: PO_4^{3-} concentration was higher in LWS than HWS upstream (till 9.5 km, *i.e.*, in the outcrop zones of Sologne sands and clays and Orléanais formation), and lower in LWS than HWS downstream (from 12.3 km, *i.e.* in the outcrop zone of Pithiviers limestones followed by Gâtinais molasse).

The DOC values ranged from 16 to 25 $mg_C\ L^{-1}$, the highest values founded upstream in the outcrop zones of Sologne sands and clays and Orléanais marls and sands (0 – 3 km). The DOC values showed a general downgradient decrease with higher values in LWS compared to HWS. The DOC variations were found to be inversely correlated to DIC variations (correlation coefficient of – 0.94; Suppl. Inf. Table 6), indicating different carbon sources in the river.

4.3 Stream water uranium

The spatial and seasonal variations of U concentration and AR in the Œuf river were illustrated on Figure 5. Data were reported in Suppl. Inf. Table 4.

4.3.1 Spatial and seasonal variation

In the Œuf river, U concentration overall increased upstream to downstream, roughly varying by 3 orders of magnitude between 0.02 µg L^{-1} and 19.3 µg L^{-1}. In parallel, AR decreased by half upstream (1.06) to downstream (0.41).

Firstly, the longitudinal variations of U concentration and AR found in the Œuf river during LWS (Low Water Season) were described. Upstream to downstream, the stream displayed various U features (Figure 5**Erreur ! Source du renvoi introuvable.**):

- In the outcrop zone of Sologne sands and clays followed by Orléanais marls and sands (B+C1; 0 – 3 km), U concentration was relatively low (0.02 – 0.9 µg L^{-1}), and AR was less but close to 1 (0.90 – 0.97);
- In the outcrop zone of Orléanais marls and limestones (C2; 3 – 9.5 km), U concentration increased and ranged from single (6.6 µg L^{-1}) to double (12.4 µg L^{-1}), and AR remained close to 1 and slightly decreased (0.87 – 0.90);
- In the outcrop zone of Pithiviers limestones (E; 10.9 – 23.1 km), the stream exhibited the highest values of U concentration which varied in a narrow range (15.0 – 19.3 µg L^{-1}) and AR significantly decreased (0.44 – 0.51);
- In the outcrop zone of Gâtinais molasse (F; 23.1 – 32 km), U concentration decreased and varied in a narrow range (12.2 – 13.7 µg L^{-1}), and AR slightly decreased and displayed the lowest values (down to 0.41).

Secondly, U and AR longitudinal profiles were compared according to the hydrological season. While U concentration and AR exhibited similar longitudinal trends together in HWS and LWS, noticeable differences were shown based on the amplitude of their variations: U concentration was systematically lower in HWS than LWS, while AR showed the contrary. Upstream to downstream U concentration exhibited two peak values. In the outcrop zone of Orléanais marls and limestones (3 – 9.5 km), the maximum of U concentration was 12.4 µg L^{-1} in LWS and 2.5 µg L^{-1} in LWS (*i.e.*, 6 times less). In the outcrop zone of Pithiviers limestones (10.9 – 23.1 km), the maximum U concentration was 19.3 µg L^{-1} in LWS and 11.5 µg L^{-1} in HWS (*i.e.*, almost 2 times less). Also, a downgradient shift was observed between U peaks in HWS and LWS: first U peak occurred at 4.9 km in LWS and 8.2 km in HWS, and second peak U occurred at 14.1 km in LWS and 17.8 km in HWS. Similarly, the decrease of U concentration was observed from 17.8 to 24.9 km in LWS, and from 24.9 to 29.5 km in HWS.

The outcrop zone of Pithiviers limestones (10.9 – 23.1 km) was the river stretch that registered the greatest changes in both U concentration and AR whatever the hydrological season. In HWS, the observation of a sharp rise in U concentration (from 2.1 to 11.5 µg L^{-1}) was inversely related to a sharp fall in AR (from 1.0 to 0.54). In LWS, U concentration displayed high values of U concentration and inversely low AR was soon as the stream water re-emerged (at 12.3 km in June and 14.1 km in September and December).

Regarding the four tributaries (T1 to T4) discharging in the Œuf river (in HWS only), U concentration and AR exhibited variations in the ranges 0.11 – 4.2 µg L^{-1} and 0.81 – 1.0, respectively.

Whatever the hydrological season, U concentration was well correlated with several parameters and analytes (Suppl. Inf. Table 6): positively with EC, DIC, NO_3^-, Mg, Ca, Sr, Ba and Se (coefficient above 0.8), and negatively with DOC and AR (coefficient below – 0.8). The positive and good correlation coefficient between U and EC, DIC and Ca indicated that U occurrence in the stream water was related to carbonate dissolution, as expected in sedimentary basin (Smedley & Kinniburgh, 2023). The positive relationships of U to Se (0.93), NO_3^- (0.83) and to a lesser extent to SO_4^{2-} (0.48) suggested either a common origin in the river catchment (*e.g.*, a specific mineralization) or a concomitant transfer (the way they were supplied to the river is the same). The negative relationship of U to AR (– 0.89) indicated that the more the water got enriched in U, the more U was depleted in ^{234}U.

4.3.2 U aqueous species

The results of U speciation modelling with PHREEQC are reported in Suppl. Inf. Table 7. In the Œuf river, U was found in its oxidized form U(VI) as expected in freshwater. Whatever the hydrological season, U was found to form inorganic complexes $UO_2(CO_3)_2^{2-}$, $UO_2(CO_3)_4^{3-}$ and $UO_2(CO_3)$. In LWS only, U was occasionally found in forms of UO_2^{2+} and UO_2OH^+. These U aqueous species were in agreement with the ones expected in freshwater (Lartigue et al., 2020; Markich, 2002), *i.e.*, hydroxyl complexes ($UO_2(OH)_n^{(2-n)+}$) and carbonate complexes ($Ca_nUO_2(CO_3)_3^{(4-2n)-}$). Also, U was found to complex with phosphate anion to form $UO_2(HPO_4)_2^{2-}$. Although phosphate is an inorganic ligand currently occurring in freshwater (Markich, 2002), the stability of complex with U under natural conditions is debated (Sandino & Bruno, 1992; X. Wang et al., 2019).

4.4 Groundwater chemistry

The groundwater data relative to BLAS units are presented in Suppl. Inf. Table 5. Between the different BLAS units, EC values varied in a narrow range, between 691 and 554 µS cm^{-1} (in average), that fitting well with European limestone aquifer (Wendland et al., 2008) (from 95 to 1,146 µS cm^{-1}). Also, Ca concentration varied in a narrow range, between 95 and 111 mg L^{-1} (in average), which fitted well with the values expected in limestone aquifers (Wendland et al., 2008) (from 66 to 122 mg L^{-1}). The values of ORP weere available in groundwater GW3 only, and it showed fluctuations with time (from 100 to 268 mV).

Differences between BLAS units were seen regarding the anion concentration. The concentration of Cl^- showed high values in the groundwater GW2 (49 mg L^{-1} in average) compared to GW1, GW3 and GW4 (22 and 23 mg L^{-1} in average). The concentration of NO_3^- was very low in GW4 (0.55 mg L^{-1} in average), it showed much higher concentration in GW1 (29 mg L^{-1} in average), and the highest values were found in GW2 and GW3 (44 and 45 mg L^{-1} in average). In the water extracted from Pithiviers limestones (GW2 and GW3), NO_3^- concentration occasionally exceeded the WHO guideline for drinking-water purpose (50 mg L^{-1}).

In BLAS units of interest, U concentration ranged from 7.3 to 12 µg L^{-1} (in average), this level of U concentration being in accordance with that expected in limestone aquifers (Bonotto & Andrews, 2000; Smedley et al., 2006) (*i.e.*, below 15 µg L^{-1}). The values of AR were systematically below 0.5 (from 0.32 to 0.45 in average).

5 Discussion

5.1 River-groundwater continuum

5.1.1 Hydrogeological approach

In this section we examined the origin of the water supplied to the Œuf river according to the hydrogeological settings.

In LWS, the Œuf river was shown gaining or losing water when flowing above Orléanais formation (0 – 9.5 km) and at the beginning of the outcrop zone of Pithiviers limestones (before 14.1 km). The stream was only gaining water above Sologne sands and clays (0 – 3 km) and after Pithiviers limestones changed from confined to unconfined aquifer (from 14.1 km). The way the Œuf river interacted with these aquifers is typical of headwater streams flowing at head catchment and hydraulically connected to groundwater (Khan & Khan, 2019). In the period of negative efficient rainfall (rainfall level below evapotranspiration in LWS), the flow of the Œuf river was transient, thus depending on groundwater discharge and water table fluctuations. In HWS, the rainfall and the surface runoff led to maintain a continuous flow along the stream riverbed.

To characterize the interaction between the Œuf river flowing on the surface and the groundwater of the different BLAS units outcropping in the river catchment, we first examined the existing potentiometric lines (BRGM, 1995; Verley, Brunson, Verjus, & Cholez, 2003). Although available, this information was not appropriate to the space scale of our field observations. Based on our observations, we considered the Œuf river as an outlet for aquifer discharges from Sologne sands (0 – 3 km), Orléanais marls and limestones (3 – 9.5 km) and Pithiviers limestones (10.9 – 23.1 km).

5.1.2 Geochemical approach

In this section, the influence of the geology and the hydrological season on the stream water chemistry of the Œuf river was examined.

The lower values and the lower amplitude observed for EC and major chemical specie concentrations (DIC, SO_4^{2-}, NO_3^-, Cl^-, Ca) in HWS compared to LWS indicate a water supply being less mineralized. This decreasing degree of mineralization in HWS was attributed to the contribution of surface runoff and rainfall to the river water. To focus on the interaction between river and groundwater, the stream water chemistry in LWS was further examined only. The longitudinal profile of EC indicated a stream water increasingly mineralized upstream to downstream. The EC values were well and positively correlated with DIC and Ca, and the other alkaline earth elements Mg and Sr. When flowing on Orléanais marls and limestones (3 – 9.5 km) and Pithiviers limestones (3 – 23.1 km), the Œuf river got noticeably enriched in DIC and Ca. The Ca level in the stream water (above 100 mg L^{-1}) fitted relatively well with the range of values found in the corresponding aquifer units (95 – 111 mg L^{-1} in average in GW1, GW2 and GW3; Suppl. Inf. Table 5). Therefore, the observation of an increasing mineralized stream water gave the evidence of an aquifer discharge that mainly consisted in limestones and where carbonate dissolution took place. In the most downstream zone, *i.e.*, where outcrop Gâtinais molasse (23.1 – 32 km), the stream water records a sharp increase of Cl^-, Br^-, Mg, Na, K and Sr concentrations. That change was attributed to the groundwater discharge from this geological formation, although it was only defined as an aquitard.

When plotting the molar ratios Mg/Ca *vs* Sr/Ca (Figure 6), differences were seen in the stream water depending on the geology. The stream water flowing in the outcrop zone of Sologne sands and clays followed by Orléanais marls and sands distinguished from that flowing downstream: the ratio Mg/Ca was relatively high (above 3) in this zone compared to others (Mg/Ca below 1.5). From Orléanais marls and limestones to Gâtinais molasse, the increasing trend of Mg and Sr concentrations indicated that water supplied to the stream got enriched in these alkaline earth metals. That possibly reflected an

ageing effect: the more the groundwater was aged, the more it contained elements that have been solubilized through the carbonate dissolution in limestone aquifer. That was evidenced by the difference observed between Mg/Ca molar ratio of the groundwater extracted from BLAS units (Suppl. Inf. Table 5): it was higher in Orléanais limestones deposited in Burdigalian (0.073 at GW1), compared to Pithiviers limestones dated from Aquitanian (0.083 at GW2).

The distribution between the dissolved carbon species gave additional information on the water origin in the stream. Nearby the spring located in the Orléans Forest, the highest DOC values indicated an enrichment of organic species attributable to the leaching of the surrounding forest soils (in form of soluble fulvic and humic substances, typically). Downgradient, as the stream water got enriched in DIC it got depleted in DOC (correlation factor of – 0.94; Suppl. Inf. Table 6). The DIC increase was taken as an indicator of groundwater discharge from the limestone aquifers interacting with the stream. Therefore, the inverse relationship between DIC and DOC gave an indication of the longitudinal variation of the water supply: upstream the stream water contained mostly soluble organic species inherited from the leachate of organic soils, while downstream the stream water acquired inorganic characteristics from the limestone aquifer discharge.

5.2 Origin of U in the Œuf river

5.2.1 Atypical feature of U

In the Œuf river, U concentration widely varied, almost by 3 orders of magnitude (from 0.02 to 19.3 µg L^{-1}). The maximum value detected in the Œuf river exceeded by 100 times the worldwide riverine value (Palmer & Edmond, 1993) (0.19 µg L^{-1}), it encompassed most of the natural waters (Salminen et al., 2005; Smedley & Kinniburgh, 2023) (generally U below 4 µg L^{-1}), including those impacted by anthropogenic U sources (Markich, 2002) (*e.g.*, mining activities). Important longitudinal fluctuations were found in headwater streams or small streams, as they were more liable to register hydrological fluctuations deriving from precipitations and groundwater discharge (Bagard et al., 2011; Durand et al., 2005; Navarro-Martínez et al., 2020). A 1000-fold variation in longitudinal U concentration was documented in areas displaying geological heterogeneities (Durand et al., 2005; Grzymko, Marcantonio, McKee, & Mike Stewart, 2007; Saari et al., 2007). The combination of longitudinal amplitude (up to 10 or 100-fold) with elevated U concentration (above 20 µg L^{-1}) has been occasionally observed in streams draining specific areas displaying localized U mineralization. This was the case of the Llobregat river (Spain) which got enriched in U when draining lignite formations (Camacho et al., 2010) (from 1.6 to 21 µg L^{-1}), another example was given by the Platte River in Colorado (United States) where headwaters got enriched in U by draining uraniferous rocks (Snow & Spalding, 1994) (from 0.27 to 31.7 µg L^{-1}). Similarities were found with U enrichment in streams affected by U release from anthropogenic activity. Examples were given by streams draining U mining areas in operation in Kazakhstan and Kyrgyzstan (Uralbekov et al., 2014) (U varied from 1.9 to 39.5 µg L^{-1}), or being no longer in operation in France (Y. Wang et al., 2013) (U varied from 2.9 to 30.9 µg L^{-1}).

In the Œuf river, AR values varied by almost 3-fold (from 0.411 to 1.06). In freshwaters, AR generally exceeds 1, the averaged riverine AR value being estimated at 1.17 (François Chabaux et al., 2001). The excess of ^{234}U activity regarding ^{238}U is a consequence of ^{234}U production mode (alpha disintegration) leading to its preferential solubilisation during rock weathering. A single example of AR below 1 in a stream was reported, corresponding to the Strengbach headwaters (France), where AR displayed 0.996 at the lowest (Riotte & Chabaux, 1999). The observation of extreme low AR values founded downstream in the Œuf river (AR below 0.6) has no equivalent in freshwater around the world. The scarcity of AR values below 1 reported for freshwater in literature is possibly due to a lack of U and AR investigations conducted in headwater streams.

The Œuf river is a small stream that receives water through groundwater discharge. In this section U characteristics were first examined in the groundwater of BLAS units that outcrop in the river catchment (Suppl. Inf. Table 5). For reminder, the groundwater data of BLAS units were acquired through a national survey program and not through the present study. Groundwater extracted from Orléanais formation and Pithiviers limestones exhibited AR below 0.4 (GW1 and GW3), indicating an extreme ^{234}U deficit with respect ^{238}U. The ubiquous observation of extreme ^{234}U deficit in three boreholes surrounding the Œuf river catchment (GW1, GW3 and GW4 in Figure 1) suggested that low AR might occurred at a regional scale and was a characteristic of BLAS reservoir. If so, that would differ from previous works which documented AR nearby 0.5 in groundwater at a local scale due to specific hydrogeological settings (Abdul-Hadi et al., 2001; Kaufman et al., 1969). Groundwater with AR nearby or below 0.5 was documented in a variety of hydrogeological settings (Abdul-Hadi et al., 2001; El-Aassy et al., 2015; Kaufman et al., 1969). To explain ^{234}U deficit in groundwater, several factors were pointed out based on field settings or laboratory experiments (Andersen, Erel, & Bourdon, 2009; Bonotto & Andrews, 2000): a change in the redox conditions (Osmond & Cowart, 1976; Osmond et al., 1983), an increasing rate of weathering in karstic limestones (Kaufman et al., 1969), a lack of U renewal during rock weathering (Kumar et al., 2016) and a leaching of surface and subsurface horizons that already have experienced ^{234}U loss (Israelson et al., 1997; Milena-Pérez et al., 2021; Riotte & Chabaux, 1999). The ground catchment of the Œuf river was likely to fulfil these conditions: karstic limestones are present at its top and groundwater is expected to oxidize when crossing the river-groundwater boundary. Regarding the Œuf river, the detection of low AR (below 0.5) in the outcrop zone of Pithiviers limestones supported the evidence of a stream hydraulically connected to aquifer.

The Œuf river received U when flowing in the outcrop zones of Orléanais marls and limestones and Pithiviers limestones. Regarding AR values, the feature of U contribution was different: U was highly depleted in ^{234}U (AR below 0.5) in the zone of Pithiviers limestones, while it was slightly depleted in the zone of Orléanais marls and limestones (AR nearby 1). This difference was not seen when regarding groundwater characteristics since both aquifers displayed low AR (below 0.4). That AR difference in the stream water possibly took its origin in local and specific hydrogeochemical settings, as it has been seen in the vicinity of surface and subsurface soil horizons (Israelson et al., 1997; Riotte & Chabaux, 1999). If considering that ^{234}U depletion is the fate of U feature in BLAS groundwater, that AR difference would provide an age marker: the more the stream water is depleted in ^{234}U, the more it is supplied by old groundwater.

5.2.2 Influence of geology and hydrology

The most elevated U concentrations were detected in the Œuf river when flowing on the Orléanais marls and limestones (12.4 µg L^{-1}) and Pithiviers limestones (19.3 µg L^{-1}). Regarding U concentration in these aquifers (Suppl. Inf. Table 5), Orléanais limestone formation (GW1) displayed similar U concentration (11 µg L^{-1} in average) and Pithiviers limestones (GW3) lower U concentration (7 µg L^{-1} in average). In limestone aquifer, U concentration was expected to be rather low (Smedley & Kinniburgh, 2023; Smedley et al., 2006), not exceeding 10 µg L^{-1}. However, if interacting with U mineralization, U concentration in the groundwater can be much higher (Smedley & Kinniburgh, 2023). In the aquifers interacting with the Œuf river, *i.e.*, Orléanais formation and Pithiviers limestones, U concentration was nearby or lower than in surface river and did not display noticeable U level. Therefore, the elevated U concentration founded in the stream waters could have resulted from specific hydrogeochemical settings (oxidizing conditions typically) in combination with localized U mineralization.

Field observations pointed out the dependence of the Œuf river flow to groundwater discharge and rainfall. In LWS, stream water was permanent nearby the stream spring area (presence of Sologne

sands) as well as in the area where Pithiviers limestone aquifer discharged water to form a continuous flow. The stream hydrology changed in HWS with rainfall, surface runoff and groundwater discharge maintaining a continuous flow along the entire riverbed. On the Beauce Plateau, the discharge rate of streams was mainly controlled by the water table level. The variation of U characteristics was taken as an indicator of the groundwater outflow into the Œuf river. In the zone where Pithiviers limestones changed from confined to unconfined groundwater, thus supporting river-groundwater interaction, in LWS the stream water displayed an hydrochemical facies typical of old water ($Ca > 100$ mg L^{-1}, $EC > 600$ µS cm^{-1}) with elevated U concentration ($U > 15$ µg L^{-1}) and low AR (below 0.5). In HWS, the stream water chemistry indicated younger water ($Ca < 70$ mg L^{-1}, $EC < 400$ µS cm^{-1}) with lower U concentration and an AR tending to 1.

In HWS, the influence of tributaries was examined by comparing U concentration upstream and downstream the first and last tributary intersection with the Œuf river (*i.e.*, at 8.2 and 12.3 km). In this river stretch, the concentration of U showed a slight decrease (from 2.52 to 2.10 µg L^{-1}). In parallel, AR remained similar and nearby 1 (from 1.03 to 1.00). Thus, the tributaries appeared to exert a minor control on U characteristics of the Œuf river. They rather diluted U concentration of the main stream and their role as potential U supplier was discarded. The systematic decrease of U concentration in stream waters indicated a dilution process attributable to precipitations as the rainwater is known to contain low U level (1.7 ng L^{-1}) (Tsumura, Okamoto, Takaku, & Yamasaki, 1995). This influence of hydrological season on U concentration is typical of small streams as they are more liable to register changes induced by rain (Saari, Schmidt, Huguet, & Lanoux, 2008).

In the outcrop zone of Pithiviers limestones (10.9 – 23.1 km), U was mainly present in the stream in form of UO_2^{2+} – CO_3^{2-} complexes (92.6 – 98.8 %; Suppl. Inf. Table 7). These highly soluble complex are typical of freshwater draining sedimentary basin made of limestones (F. Chabaux et al., 2008; Palmer & Edmond, 1993; Smedley & Kinniburgh, 2023), and leading to an enhancement of U mobility. The formation of highly soluble complexes of U with carbonates possibly favoured the occurrence of elevated level of U concentration and U mobility in the Essonne river valley.

5.2.3 U source(s) in the ground

In this section a review was done on the geological settings potentially involved in the observation of elevated U in the Œuf river. This examination was enlarged at the scale of the head catchment of the Essonne river valley, since elevated U concentration (10.5 µg L^{-1}) was also documented in another stream (Salpeteur, 2010), the Rimarde river. As the Œuf river, the Rimarde river originates in the Orléans Forest, it crosses the same geological sequence and intersects the Œuf river (the Essonne river originates from that confluence).

The source(s) of U were discussed regarding selenium (Se), another trace element that displays similar geochemical behaviour to U (*i.e.*, redox sensitive mobility), and for which an anomaly occurrence was reported in the Essonne valley. In the Œuf river, a good correlation coefficient is found between U and Se concentrations (0.93; Suppl. Inf. Table 6), indicating a common source. Both elements are generally found in association in organic rich materials (Bullock & Parnell, 2017; Meunier, Bruhlet, & Pagel, 1992), where reducing conditions prevail and are favourable to sulphur precipitation. In the redox barrier (typically an aquifer area where occurs a change from aerobic to anaerobic conditions), U and Se tend to accumulate and can be found in form of uraninite (UO_2) and ferrosilite (Fe_2Se), respectively. The increasing SO_4^{2-} concentration in the stream water concomitantly with U and Se enrichment of the stream water evoked sulphur oxidation and consecutive mineral dissolution. It is likely that U and Se accumulated in organic rich deposits within the continental deposits constituting BLAS and that oxidizing conditions led to their release through the water-rock interaction within the aquifer.

Therefore, evidence or proof of U and Se accumulation in the ground and the aquifer hosted rock was searched in the documentation relative to BLAS and adjacent formations.

Regarding BLAS and its adjacent formations from deep to surface, a variety of organic materials have been evidenced within these continental formations thus providing good candidates to concentrate U and Se. At the basis of BLAS, Ypresian formation (lower stage of Eocene) consists in lignite layer where U and Se were shown to concentrate (Gaillard, 2017; Gaillard & Garnier-Séréno, 2017) : 18.5 and 29 µg kg^{-1} for U and Se, respectively. The occurrence of lignite was also reported in Etampes limestones (Chery & Rouelle-Castrec, 2004). Since both formations do not outcrop at the head of the Essonne river valley, they could not interact directly with the streams flowing on the surface, *i.e.*, the Œuf and Rimarde rivers. If U and Se derived from these deep formations, they have been necessarily transported upward through leakage transfer. At the head of the Essonne catchment, the formation of Sologne sands and clays is known to overlay a peat layer. The Sologne sands are of granitic detrital origin and consist in heavy minerals (Etienne & Larue, 2011; Gigot, 1984), possibly containing U at non negligible level. When infiltrating, meteoric water would have solubilized U by grain leaching and then the expected reducing peat layer would have trapped U and Se (Bullock & Parnell, 2017; Cumberland et al., 2016), in a way similar to roll-front mineralization (Campbell, Gallegos, & Landa, 2015; Meunier, Bruhlet, & Pagel, 1992; Van Berk & Fu, 2017). Below the peat layer, the limestone dissolution of Orléanais carbonate formation would have provided the carbonate that promoted highly soluble and easily mobilizable uranyl complexes. Therefore, the water table fluctuation would have been responsible of U and Se trapping and release to the stream water. The ground catchment of the Œuf river is known to display a significant karstic network (Lorain, 1973), that is confirmed by the presence of palaeokarsts inside the Pithiviers limestones (see boreholes B3 and B4 on the Suppl. Inf. Figure 1). These palaeokarsts are filled by sandy detrital material probably corresponding to Sologne sands that would have provided an additional U source within the carbonate formation.

Regarding AR values in the Œuf river and the groundwater of BLAS units, U depleted in ^{234}U was present in both surface and ground waters. In general, a deficit of ^{234}U in groundwater implies an intense dissolution in zones of high permeability where the preferential leaching of U leaves behind rocks with ^{234}U deficit regarding ^{238}U (Abdul-Hadi et al., 2001; Kaufman et al., 1969). This could explain the observation of low AR (< 0.4) founded in Orléanais and Pithiviers limestone aquifers. Also it can be interpreted in terms of lack of U renewal in U accumulation in ground material (Milena-Pérez et al., 2021; Osmond & Cowart, 1976; Osmond et al., 1974): ground material that experienced a loss in ^{234}U is not compensated by the arrival of undepleted material. That could explain the difference in ^{234}U observed upstream and downstream the Œuf river. Above Orléanais limestones the stream water got enriched in U (12.3 µg L^{-1}) with AR nearby 1 (0.90), while it got enriched in U (19.3 µg L^{-1}) with lower AR (0.46) above Pithiviers limestones (Suppl. Inf. Table 4). At the upstream part of Œuf river, AR nearby 1 indicated that ground material had experienced moderate loss in ^{234}U (in case of a common U source) or had been compensated by the renewal of undepleted U (in case of multiple U sources). In case of multiple U sources, the formation containing undepleted U is expected to be the Sologne sands and clays that overlays Orléanais marls and sands. Again, this granitic detrital sand consists in heavy minerals (Etienne & Larue, 2011; Gigot, 1984), thus possibly contains U available for leaching by meteoric water infiltration. The disappearance of this geological formation in the first km of the Œuf river (< 3 km) would have explained the lack of undepleted U renewal downstream.

5.2.4 Influence of nitrate

Pending a direct identification of U source(s) in the ground catchment of the Œuf river, the other possible factors causing U enrichment in surface and groundwater were examined. Enrichment in U of surface and groundwater might have resulted from a direct contribution (of anthropogenic or geogenic

origin) or a change in U mobility owing to its redox sensitivity. The presence of nitrate is one of the factors leading to U enhancement in surface and groundwater, as it was shown in agricultural areas (Liesch, Hinrichsen, & Goldscheider, 2015; Lyons et al., 2020). Since nitrate displayed elevated level of concentration (> 20 mg L^{-1}) together in the surface and the ground waters of the Œuf river catchment, its influence was further discussed below.

In the Œuf river, the good and positive relationship of U to NO_3^- (correlation coefficient of 0.83; Suppl. Inf. Table 6) indicated a common source (synthetic nitrate fertilizer application) or was the result of a concomitant transfer to the stream (here aquifer discharge). In case of a common source, the application then solubilization of synthetic nitrate in soils would have released U in agricultural wastewater (Gardner et al., 2022). Although this was shown to generate detectable U enrichment in water up to a few micrograms per litre elsewhere (Lyons et al., 2020), it seemed unlikely to be the sole factor causing the observed U increase in the Œuf river (*i.e.*, 1000-fold increase, max. 19.3 µg L^{-1}). To date, no evidence is given in literature to link ^{234}U deficit to fertilizer application. It is even the contrary: AR is expected to tend to 1 in case of nitrate fertilizer influence (Böhlke, Verstraeten, & Kraemer, 2007; Milena-Pérez et al., 2021). Therefore, the hypothesis of fertilizer application as a direct U contribution of U in the Œuf river was discarded. Hence, the concomitant increase U and NO_3^- observed in LWS in the stream when flowing on Pithiviers limestones reflects a common water supply through groundwater discharge.

The presence of nitrate in groundwater is known to alter U solubility by oxidative dissolution of reduced U(IV) minerals present in aquifer materials (Nolan & Weber, 2015) or in subsurface soil horizons (Hee, Komlos, & Jaffé, 2007; W. M. Wu et al., 2010). Thereby, NO_3^- presence in groundwater induces U enrichment by modifying the redox conditions which in turn enhances U mobility (Banning, Demmel, Rüde, & Wrobel, 2013b; Coyte, Singh, Furst, Mitch, & Vengosh, 2019). Generally, the causal relationship between NO_3^- and U concentrations in groundwater is not easy to establish (Coyte et al., 2018; Riedel & Kübeck, 2018; Rosen et al., 2019). In groundwater of BLAS units, Pithiviers limestones exhibited relatively high NO_3^- concentration in average (> 40 mg L^{-1} in GW2 and GW3; Suppl. Inf. Table 5). In BLAS shallow aquifers, the contamination by nitrogen (and other pesticides) is known since decades (Berger et al., 1976; Desprez, 1983). The presence of nitrate at elevated concentration level reflected the vulnerability of shallow groundwater to surface land utilization. The intensive agriculture requests application of large quantity of synthetic fertilizers containing nitrate. Thus, the presence of nitrate in shallow groundwater is a marker of surface water characteristics. Shallow aquifer displaying surface water features is possibly affected by oxidizing conditions during water recharge. The presence of nitrate indicates a lack of denitrification in the aquifer water during recharge. Therefore, the presence of nitrate is an indicator of groundwater oxidizing features. In the Œuf river ground catchment, a groundwater oxidization was likely to promote U solubilization from ground materials. When the stream received back groundwater, it also got enriched in nitrate and U.

In groundwater affected by nitrate inputs, the pyrite oxidation was shown to participate to the denitrification (Zhang et al., 2012). In case of U and Se association in U mineralization of roll-front type, Se is expected to follow U geochemical behaviour (Bullock & Parnell, 2017). In reducing organic materials, U and Se together concentrate in reducing barrier corresponding to sulphur precipitation. Sulphur oxidation due to nitrate presence possibly promotes the release of U and Se associated with sulphur (Houben, Sitnikova, & Post, 2017). In the Œuf river, the positive relationship of U to Se, NO_3^- (correlation coefficient above 0.8; Suppl. Inf. Table 6) and SO_4^{2-} in a lesser extent (correlation coefficient of 0.43) supported the hypothesis of U and Se association in reducing organic ground material and their consecutive release due to nitrate presence. The Œuf river registered a decrease in U concentration and AR while NO_3^- was increasing when the stream was entering the outcrop zone of

Gâtinais molasse in LWS. The groundwater discharge in this zone was already discussed and was shown to be different from upstream, *i.e.*, in the outcrop zone of Pithiviers limestones: the discharged groundwater was shown to be more mineralized. Therefore, this change in U concentration and AR possibly indicated a specific feature of the aquifer discharge.

5.3 Tracking the aquifer discharge

In the Œuf river, the stream water was shown to derive from both groundwater discharge and surface runoff, the relative proportion of these two water components varying through time and along the river profile. In HWS, the variation of the stream water chemistry in the outcrop zone of Pithiviers limestones was shown to result from the river-groundwater interaction. Then this river stretch (10.9 – 23.1 km) was considered as a mixing zone between two water components: water component 1 corresponding to the groundwater discharge, and water component 2 corresponding to the stream water coming from upstream (Table 1). The characteristics of the groundwater discharge (water component 1) were given by the stream water collected at R7 (14.1 km) in LWS, and the characteristics of the upstream stream water (water component 2) by the stream water collected at R6 (12.3 km) in HWS. Here the geochemical characteristics of the groundwater discharged in this zone were assumed to remain unchanged between LWS and HWS.

Several analytes measured in this study have shown their ability to track the influence of river-groundwater interaction on the stream water chemistry: EC, DIC, Cl^-, Br^-, NO_3^-, SO_4^{2-}, Ca, Mg, Sr, Ba, Na, K, Se, U and AR. These indicators were tested to identify those suitable for quantifying groundwater supply in HWS based on the data acquired in March 2020. Amongst them, only U isotopes and Se have provided appropriate hydrogeochemical tools, as indicated by the linear distributions between the two water components 1 and 2 (Figure 7). Then the relative proportion of groundwater volume to the stream was calculated upstream to downstream: from 12 ± 1 % at 14.1 km (R7) to 59 ± 4 % at 17.8 km (R10), corresponding to U increasing rate of 13 % per km.

This study further supports the use of U isotopes to quantitatively track groundwater supply in stream water as it was already demonstrated elsewhere, in combination with the major elements Cl^- and Na^+ (Navarro-Martínez et al., 2020), and Sr isotopes (Gardner et al., 2022; Riotte & Chabaux, 1999). By using U in combination with Se as tracers of the river-groundwater continuum, this study first demonstrates the suitability of combining two redox sensitive trace elements, *i.e.*, U and Se.

6 Conclusion

Atypical U characteristics were found in the headwater stream of the Essonne river, *i.e.*, the namely Œuf river: the stream water exhibited elevated U concentration up to 19.3 µg L^{-1} (which exceeded by 100-fold the average worldwide riverine concentration of 0.19 µg L^{-1}), and low AR down to 0.41 (which was almost the third of the expected value in freshwater, *i.e.*, 1.17). By reporting these atypical U characteristics, this study gives new insight on geogenic U and AR fluctuations in natural rivers. The Œuf river was shown to get enriched in U when interacting with Beauce limestone aquifer. Elevated U concentration (above 15 µg L^{-1}) was found in association with low AR (below 0.5) when the stream water was supplied by groundwater in the zone where limestone aquifer changed from confined to unconfined. Taking advantage of changes in the origin of water supplied to the stream (groundwater, surface runoff) and its contrasted U and Se characteristics, the groundwater contribution was quantified to the stream water: in March 2020, the groundwater supplied from 12 to 59 % of the total water flowing in the stream. Our results demonstrate the interest of investigating geogenic U fluctuations in small streams draining catchment where outcrop heterogeneous geology. By combining U and Se, this study promotes the use of trace element sensitive to redox conditions as suitable hydrogeochemical tools to characterize the river-groundwater continuum.

Credit authorship contribution statement

M. Zebracki: conceptualization, methodology, resources, writing-original draft preparation, supervision, funding acquisition; **C. Marlin**: conceptualization, writing-review; **T. Gaillard**: conceptualization, writing-review, visualization; **J. Gorny**: methodology, resources; **O. Diez**: methodology, resources; **V. Durand**: conceptualization, visualization; **C. Lafont**: methodology, resources; **C. Jardin**: methodology, resources; **V. Monange**: visualization.

Declaration of competing interest

The authors declare that the research was conducted in the absence of any commercial or financial relationships that could be construed as a potential conflict of interest.

Acknowledgements

The authors are grateful to Dr. Christelle Courbet, Dr. Caroline Simonucci, Damien Tournieux and Dr. Claire Gréau (IRSN) for sharing relevant information relative to the study area. The authors are particularly thankful to Dr. Alkiviadis Gourgiotis (IRSN) for kindly sharing his expertise in ICP-MS measurement. Special thanks are addressed to Evelyne Barker and Anthony Julien (IRSN) for their analytical assistance during the preliminary investigations. The authors thank Louise Darricau (IRSN) and Dr. Olivier Clarisse (Moncton University, Canada) for occasional help during field and laboratory works. The authors thank Dr. Charlotte Cazala and Christophe Debayle (IRSN) for proofreading. This work was funded by the French programme NEEDS as part of the UTOPIA project. This is PATERSON, the IRSN mass spectrometry platform, contribution n°17.

Disclaim

The present publication reflects only the authors' view. Responsibility for the information and views expressed therein lies entirely with the authors.

Reference list

Abdul-Hadi, A., Alhassanieh, O., & Ghafar, M., 2001. Disequilibrium of uranium isotopes in some Syrian groundwater. *Applied Radiation and Isotopes*, *55*(1), 109–113. https://doi.org/10.1016/S0969-8043(00)00369-9

Andersen, M. B., Erel, Y., & Bourdon, B., 2009. Experimental evidence for 234U-238U fractionation during granite weathering with implications for 234U/238U in natural waters. *Geochimica et Cosmochimica Acta*, *73*(14), 4124–4141. https://doi.org/10.1016/j.gca.2009.04.020

Bagard, M. L., Chabaux, F., Pokrovsky, O. S., Viers, J., Prokushkin, A. S., Stille, P., Rihs, S., Schmitt, A. D., & Dupré, B., 2011. Seasonal variability of element fluxes in two Central Siberian rivers draining high latitude permafrost dominated areas. *Geochimica et Cosmochimica Acta*, *75*(12), 3335–3357. https://doi.org/10.1016/j.gca.2011.03.024

Balcaen, L., Bolea-fernandez, E., Resano, M., & Vanhaecke, F., 2015. Inductively coupled plasma – Tandem mass spectrometry (ICP-MS/MS): A powerful and universal tool for the interference-free determination of (ultra) trace elements – A tutorial review. *Analytica Chimica Acta*, *894*, 7–19. https://doi.org/10.1016/j.aca.2015.08.053

Banning, A., Demmel, T., Rüde, T. R., & Wrobel, M., 2013a. Groundwater uranium origin and fate control in a river valley aquifer. *Environmental Science and Technology*, *47*(24), 13941–13948. https://doi.org/10.1021/es304609e

Banning, A., Demmel, T., Rüde, T. R., & Wrobel, M., 2013b. Groundwater uranium origin and fate control in a river valley aquifer. *Environmental Science and Technology*, *47*(24), 13941–13948. https://doi.org/10.1021/es304609e

Bassil, J., Naveau, A., Fontaine, C., Grasset, L., Bodin, J., Porel, G., Razack, M., Kazpard, V., & Popescu, S. M., 2016. Investigation of the nature and origin of the geological matrices rich in selenium within the Hydrogeological Experimental Site of Poitiers, France. *Comptes Rendus - Geoscience*, *348*(8), 598–608. https://doi.org/10.1016/j.crte.2016.08.004

Berger, G., Bosch, B., Desprez, N., Letolle, R., Marce, A., Mariotti, A., & Mégnien, C., 1976. *Recherches sur l'origine des nitrates dans les eaux souterraines de la Beauce. Rapport sur la campagne de prélèvements et d'analyses du 1er semestre 1976. Rap. BRGM 76 SGN 444 BDP*.

Böhlke, J. K., Verstraeten, I. M., & Kraemer, T. F., 2007. Effects of surface-water irrigation on sources, fluxes, and residence times of water, nitrate, and uranium in an alluvial aquifer. *Applied Geochemistry*, *22*(1), 152–174. https://doi.org/10.1016/j.apgeochem.2006.08.019

Bonotto, D. M., & Andrews, J. N., 2000. The transfer of uranium isotopes 234U and 238U to the waters interacting with carbonates from Mendip Hills area (England). *Applied Radiation and Isotopes*, *52*(4), 965–983. https://doi.org/10.1016/S0969-8043(99)00151-7

BRGM. (1995). *Piézométrie du système aquifère de Beauce - Basses eaux 1994 (R38572)*.

Bullock, L. A., & Parnell, J., 2017. Selenium and molybdenum enrichment in uranium roll-front deposits of Wyoming and Colorado, USA. *Journal of Geochemical Exploration*, *180*(May), 101–112. https://doi.org/10.1016/j.gexplo.2017.06.013

Camacho, A., Devesa, R., Vallés, I., Serrano, I., Soler, J., Blázquez, S., Ortega, X., & Matia, L., 2010. Distribution of uranium isotopes in surface water of the Llobregat river basin (Northeast Spain). *Journal of Environmental Radioactivity*, *101*(12), 1048–1054. https://doi.org/10.1016/j.jenvrad.2010.08.005

Campbell, K. M., Gallegos, T. J., & Landa, E. R., 2015. Biogeochemical aspects of uranium mineralization, mining, milling, and remediation. *Applied Geochemistry*, *57*, 206–235.

https://doi.org/10.1016/j.apgeochem.2014.07.022

Cary, L., Joulian, C., Battaglia-Brunet, F., & Decouchon, E., 2018. Arsenic et Sélénium dans les eaux souterraines de Beauce et de Sologne - caractérisation des eaux souterraines sur 26 communes. In *BRGM/RP-67590-FR*.

Chabaux, F., Bourdon, B., & Riotte, J., 2008. Chapter 3 U-Series Geochemistry in Weathering Profiles, River Waters and Lakes. *Radioactivity in the Environment*, *13*(07), 49–104. https://doi.org/10.1016/S1569-4860(07)00003-4

Chabaux, F, Riotte, J., & Dequincey, O., 2003. U-Th-Ra fractionation during weathering and river transport. *Reviews in Mineralogy and Geochemistry*, *52*, 533–576. https://doi.org/10.2113/0520533

Chabaux, François, Riotte, J., Clauer, N., & France-Lanord, C., 2001. Isotopic tracing of the dissolved U fluxes of Himalayan rivers: Implications for present and past U budgets of the Ganges-Brahmaputra system. *Geochimica et Cosmochimica Acta*, *65*(19), 3201–3217. https://doi.org/10.1016/S0016-7037(01)00669-X

Chery, L., & Rouelle-Castrec, M., 2004. Les occurrences de sélénium dans les forages d'alimentation en eau de la région parisienne: origine et perspectives d'étude. *Géologie et Hydrogéologie Du Bassin de Paris. Avancées et Perspectives, 16-17 Novembre*, 197–204.

Chkir, N., Guendouz, A., Zouari, K., Hadj Ammar, F., & Moulla, A. S., 2009. Uranium isotopes in groundwater from the continental intercalaire aquifer in Algerian Tunisian Sahara (Northern Africa). *Journal of Environmental Radioactivity*, *100*(8), 649–656. https://doi.org/10.1016/j.jenvrad.2009.05.009

Condon, D. J., McLean, N., Noble, S. R., & Bowring, S. A., 2010. Isotopic composition (238U/235U) of some commonly used uranium reference materials. *Geochimica et Cosmochimica Acta*, *74*(24), 7127–7143. https://doi.org/10.1016/j.gca.2010.09.019

Coyte, R. M., Jain, R. C., Srivastava, S. K., Sharma, K. C., Khalil, A., Ma, L., & Vengosh, A., 2018. Large-Scale Uranium Contamination of Groundwater Resources in India. *Environmental Science and Technology Letters*, *5*(6), 341–347. https://doi.org/10.1021/acs.estlett.8b00215

Coyte, R. M., Singh, A., Furst, K. E., Mitch, W. A., & Vengosh, A., 2019. Co-occurrence of geogenic and anthropogenic contaminants in groundwater from Rajasthan, India. *Science of the Total Environment*, *688*, 1216–1227. https://doi.org/10.1016/j.scitotenv.2019.06.334

Cumberland, S. A., Douglas, G., Grice, K., & Moreau, J. W., 2016. Uranium mobility in organic matter-rich sediments: A review of geological and geochemical processes. *Earth-Science Reviews*, *159*, 160–185. https://doi.org/10.1016/j.earscirev.2016.05.010

Desprez, N. (1983). *Etude de la stratification chimique dans la partie libre de la nappe des calcaires de Beauce (Loiret). Rap. BRGM 83 SGN 115 CEN*.

Durand, S., Chabaux, F., Rihs, S., Duringer, P., & Elsass, P., 2005. U isotope ratios as tracers of groundwater inputs into surface waters: Example of the Upper Rhine hydrosystem. *Chemical Geology*, *220*(1–2), 1–19. https://doi.org/10.1016/j.chemgeo.2005.02.016

Eary, L. E., & Jenne, E. A., 1992. *Version 4.00 of the MINTEQ geochemical code.* Retrieved from doi:10.2172/7073252

El-Aassy, I. E., El-Feky, M. G., Issa, F. A., Ibrahim, N. M., Desouky, O. A., & Khattab, M. R., 2015. Uranium and 234U/238U isotopic ratios in some groundwater wells at Southwestern Sinai, Egypt. *Journal of Radioanalytical and Nuclear Chemistry*, *303*(1), 357–362.

https://doi.org/10.1007/s10967-014-3461-y

Etienne, R., & Larue, J.-P., 2011. Contribution à l'étude des liaisons Loire-Seine: mise en évidence par l'étude des minéraux lourds de l'antécédence de la Loire en Sologne (Bassin Parisien, France). *Physio-Géo*, *5*, 269–291. https://doi.org/https://doi.org/10.4000/physio-geo.2181

Fleischer, R. L., 1980. Isotopic Disequilibrium of Uranium : Alpha-Recoil Damage and Preferential Solution Effects. *Science*, *207*, 979–981.

Gaillard, T., 2017. *Etude de sécurisation en eau potable de plusieurs communes du Sud-Est de l'Essonne. Résultats de la plateforme hydréologique de Maisse*.

Gaillard, T., & Garnier-Séréno, C., 2017. Intérêt des réseaux multi-profondeurs, exemple de la plateforme de Maisse (Essonne, France). *Géologues*, *195*, 34–37.

Gardner, C. B., Wichterich, C., Calero, A. E., Welch, S. A., Widom, E., Smith, D. F., Carey A. E., & Lyons, W. B., 2022. Carbonate weathering , phosphate fertilizer, and hydrologic controls on dissolved uranium in rivers in the US Corn Belt : Disentangling seasonal geogenic- and fertilizer-derived sources. *Science of the Total Environment*, (November), 17. https://doi.org/10.1016/j.scitotenv.2022.160455

Gigot, C., 1984. *Notice explicative de la feuille Bellegarde-du-Loiret à 1/50000*.

Gourgiotis, A., Mangeret, A., Manhès, G., Blanchart, P., Stetten, L., Morin, G., Le Pape, P., Lefebvre P., Le Coz, M., & Cazala, C., 2020. New Insights into Pb Isotope Fingerprinting of U-Mine Material Dissemination in the Environment: Pb Isotopes as a Memory Dissemination Tracer. *Environmental Science and Technology*, *54*(2), 797–806. https://doi.org/10.1021/acs.est.9b04828

Grabowski, P., & Bem, H., 2012. Uranium isotopes as a tracer of groundwater transport studies. *Journal of Radioanalytical and Nuclear Chemistry*, *292*(3), 1043–1048. https://doi.org/10.1007/s10967-011-1558-0

Gronbaek-Thorsen, F., Stürup, S., Gammelgaard, B., & Hyrup Moller, L., 2019. Development of a UPLC-IDA-ICP-MS/MS method for peptide quantitation in plasma by Se-labelling, and comparison to S-detection of the native. *Journal of Analytical Atomic Spectrometry*, *34*, 375–383. https://doi.org/10.1039/c8ja00341f

Grzymko, T. J., Marcantonio, F., McKee, B. A., & Mike Stewart, C., 2007. Temporal variability of uranium concentrations and 234U/238U activity ratios in the Mississippi river and its tributaries. *Chemical Geology*, *243*(3–4), 344–356. https://doi.org/10.1016/j.chemgeo.2007.05.024

Hee, S. M., Komlos, J., & Jaffé, P. R., 2007. Uranium reoxidation in previously bioreduced sediment by dissolved oxygen and nitrate. *Environmental Science and Technology*, *41*(13), 4587–4592. https://doi.org/10.1021/es063063b

Horwitz, E. P., Dietz, M. L., Chiarizia, R., Diamond, H., Essling, A. M., & Graczyk, D., 1992. Separation and preconcentration of uranium from acidic media by extraction chromatography. *Analytica Chimica Acta*, *266*(1), 25–37. https://doi.org/10.1016/0003-2670(92)85276-C

Houben, G. J., Sitnikova, M. A., & Post, V. E. A., 2017. Terrestrial sedimentary pyrites as a potential source of trace metal release to groundwater e A case study from the Emsland , Germany. *Applied Geochemistry*, *76*, 99–111. https://doi.org/10.1016/j.apgeochem.2016.11.019

Howard III, J. H., 1977. Geochemistry of selenium: formation of ferroselite and selenium behavior in the vicinity of oxidizing sulfide and uranium deposits. *Geochimica et Cosmochimica Acta*, *41*(11),

1665–1678. Retrieved from http://www.sciencedirect.com/science/article/B6V66-48C8JD2-VK/2/0e2f2b4c207daf16e957a55b8e63a952

Huckle, D., Ma, L., McIntosh, J., Vázquez-Ortega, A., Rasmussen, C., & Chorover, J., 2016. U-series isotopic signatures of soils and headwater streams in a semi-arid complex volcanic terrain. *Chemical Geology*, *445*, 68–83. https://doi.org/10.1016/j.chemgeo.2016.04.003

Israelson, C., Bjrck, S., Hawkesworth, C. J., & Possnert, G., 1997. Direct U-Th dating of organic- and carbonate-rich lake sediments from southern Scandinavia. *Earth and Planetary Science Letters*, (97).

Kaufman, M. I., Rydell, H. S., & Osmond, J. K., 1969. 234U/238U Disequilibrium as an aid to hydrologic study of the Floridan aquifer. *Journal of Hydrology*, *9*, 374–386.

Khan, H. H., & Khan, A., 2019. Groundwater and surface water interaction. In *GIS and Geostatistical Techniques for Groundwater Science*. https://doi.org/10.1016/B978-0-12-815413-7.00014-6

Kigoshi, K., 1971. Alpha-Recoil Thorium-234: Dissolution into Water and the Uranium-234/Uranium-238 Disequilibrium in Nature. *Science*, *173*(5), 47–48.

Kumar, A., Karpe, R. K., Rout, S., Gautam, Y. P., Mishra, M. K., Ravi, P. M., & Tripathi, R. M., 2016. Activity ratios of 234U/238U and 226Ra/228Ra for transport mechanisms of elevated uranium in alluvial aquifers of groundwater in south-western (SW) Punjab, India. *Journal of Environmental Radioactivity*, *151*, 311–320. https://doi.org/10.1016/j.jenvrad.2015.10.020

Lartigue, J. E., Charrasse, B., Reile, B., & Descostes, M., 2020. Aqueous inorganic uranium speciation in European stream waters from the FOREGS dataset using geochemical modelling and determination of a U bioavailability baseline. *Chemosphere*, *251*, 126302. https://doi.org/10.1016/j.chemosphere.2020.126302

Larue, J.-P., & Étienne, R., 2014. Évolution quaternaire de la ligne de partage des eaux entre les bassins de la Seine et de la Loire, du Perche à la Puisaye : hydrographie, structure et tectonique. *Norois*, (230), 95–108. https://doi.org/10.4000/norois.5044

Liesch, T., Hinrichsen, S., & Goldscheider, N., 2015. Uranium in groundwater - Fertilizers versus geogenic sources. *Science of the Total Environment*, *536*, 981–995. https://doi.org/10.1016/j.scitotenv.2015.05.133

Lorain, J., 1973. *Le Calcaire de Beauce: géologie, hydrogéologie, applications en construction routière et génie civil*.

Lyons, W. B., Gardner, C. B., Welch, S. A., & Israel, S., 2020. Uranium in Ohio, USA Surface Waters: Implications for a Fertilizer Source in Waters Draining Agricultural lands. *Scientific Reports*, *10*(1), 1–6. https://doi.org/10.1038/s41598-020-61922-2

Mangini, A., Sonntag, C., Bertsch, G., & Müller, E., 1979. Evidence for a higher natural uranium content in world rivers [5]. *Nature*, *278*(5702), 337–339. https://doi.org/10.1038/278337a0

Markich, S. J., 2002. Uranium speciation and bioavailability in aquatic systems: an overview. *The Scientific World Journal*, *2*, 707–729. https://doi.org/10.1100/tsw.2002.130

Martin, J.-C., Giot, D., & Le Nindre, Y. M., 1999. *Etudes préalables à la réalisaton d'un modèle de gestion de la nappe de Beauce - Geométrie du réservoir et limites de la nappe de Beauce. Rap. BRGM R 40571*.

Mathieu, D., Bernat, M., & Nahon, D., 1995. Short-lived U and Th isotope distribution in a tropical laterite derived from granite (Pitinga river basin, Amazonia, Brazil): Application to assessment of weathering rate. *Earth and Planetary Science Letters*, *136*, 703–714.

927 Meunier, J. D., Bruhlet, J., & Pagel, M., 1992. Uranium mobility in the sediment-hosted uranium
928 deposit of Coutras, France. *Applied Geochemistry*, *7*(2), 111–121. https://doi.org/10.1016/0883-
929 2927(92)90030-7

930 Michel, R. L., Kraemer, T. F., & DeWayne Cecil, L., 2009. Chapter 5.1 Surface water, unsaturated zone,
931 and glacial systems. In *Radioactivity in the Environment* (Vol. 16).
932 https://doi.org/10.1016/S1569-4860(09)01605-2

933 Milena-Pérez, A., Piñero-García, F., Benavente, J., Expósito-Suárez, V. M., Vacas-Arquero, P., & Ferro-
934 García, M. A., 2021. Uranium content and uranium isotopic disequilibria as a tool to identify
935 hydrogeochemical processes. *Journal of Environmental Radioactivity*, *227*(December 2020).
936 https://doi.org/10.1016/j.jenvrad.2020.106503

937 Navarro-Martinez, F., Salas Garcia, A., Sánchez-Martos, F., Baeza Espasa, A., Molina Sánchez, L., &
938 Rodríguez Perulero, A., 2017. Radionuclides as natural tracers of the interaction between
939 groundwater and surface water in the River Andarax, Spain. *Journal of Environmental*
940 *Radioactivity*, *180*, 9–18. https://doi.org/10.1016/j.jenvrad.2017.09.015

941 Navarro-Martínez, F., Sánchez-Martos, F., Salas García, A., & Gisbert Gallego, J., 2020. The use of
942 major, trace elements and uranium isotopic ratio (234U/238U) for tracing of hydrogeochemical
943 evolution of surface waters in the Andarax River catchment (SE Spain). *Journal of Geochemical*
944 *Exploration*, *213*(February), 106533. https://doi.org/10.1016/j.gexplo.2020.106533

945 Nolan, J., & Weber, K. A., 2015. Natural Uranium Contamination in Major U.S. Aquifers Linked to
946 Nitrate. *Environmental Science and Technology Letters*, *2*(8), 215–220.
947 https://doi.org/10.1021/acs.estlett.5b00174

948 Ollivier, P., Radakovitch, O., & Hamelin, B., 2011. Major and trace element partition and fluxes in the
949 Rhône River. *Chemical Geology*, *285*(1–4), 15–31.
950 https://doi.org/10.1016/j.chemgeo.2011.02.011

951 Osmond, J. K., & Cowart, J. B., 1976. The theory and uses of natural uranium isotopic variations in
952 hydrology. *Atomic Energy Review*, *14*(4), 621–679.

953 Osmond, J. K., Cowart, J. B., & Ivanovich, M., 1983. Uranium isotopic disequilibrium in ground water
954 as an indicator of anomalies. *Nuclear Geophysics*, *34*(I), 283–308. https://doi.org/10.1016/0020-
955 708X(83)90132-1

956 Osmond, J. K., Kaufman, M. I., & Cowart, J. B., 1974. Mixing volume calculations, sources and aging
957 trends of Floridan aquifer water by uranium isotopic methods. *Geochimica et Cosmochimica*
958 *Acta*, *38*(7), 1083–1100. https://doi.org/10.1016/0016-7037(74)90006-4

959 Osmond, J. K., Rydell, H. S., & Kaufman, M. I., 1968. Uranium Disequilibrium in Groundwater : An
960 Isotope Dilution Approach in Hydrologic Investigations. *Science*, *162*, 997–999.

961 Paces, J. B., & Wurster, F. C., 2014. Natural uranium and strontium isotope tracers of water sources
962 and surface water – groundwater interactions in arid wetlands – Pahranagat Valley, Nevada,
963 USA. *Journal of Hydrology*, *517*, 213–225. https://doi.org/10.1016/j.jhydrol.2014.05.011

964 Palmer, M. R., & Edmond, J. M., 1993. Uranium in river water. *Geochimica et Cosmochimica Acta*,
965 *57*(20), 4947–4955. https://doi.org/10.1016/0016-7037(93)90131-F

966 Parkhurst, D. L., & Appelo, C. A. J., 2013. Description of Input and Examples for PHREEQC Version 3 –
967 A Computer Program for Speciation, Batch-Reaction, One-Dimensional Transport, and Inverse
968 Geochemical Calculations. In *U.S. Geological Survey Techniques and Methods*.
969 https://doi.org/10.1097/00000446-195210000-00005

970 Pierret, M. C., Stille, P., Prunier, J., Viville, D., & Chabaux, F., 2014. Chemical and U-Sr isotopic
971 variations in stream and source waters of the Strengbach watershed (Vosges mountains,
972 France). *Hydrology and Earth System Sciences*, *18*(10), 3969–3985.
973 https://doi.org/10.5194/hess-18-3969-2014

974 Pregler, A., Surbeck, H., Eikenberg, J., Werthmüller, S., Szidat, S., & Türler, A., 2019. Increased
975 uranium concentrations in ground and surface waters of the Swiss Plateau: A result of uranium
976 accumulation and leaching in the Molasse basin and (ancient) wetlands? *Journal of*
977 *Environmental Radioactivity*, *208–209*(June), 106026.
978 https://doi.org/10.1016/j.jenvrad.2019.106026

979 Rasplus, L., 1982. *Contribution à l'étude géologique des formations continentales détritiques du Sud-*
980 *Ouest du bassin de Paris*.

981 Read, D., Bennett, D. G., Hooker, P. J., Ivanovich, M., Longworth, G., Milodowski, A. E., & Noy, D. J.,
982 1993. The migration of uranium into peat-rich soils at Broubster, Caithness, Scotland, U.K.
983 *Journal of Contaminant Hydrology*, *13*(1–4), 291–308. https://doi.org/10.1016/0169-
984 7722(93)90067-3

985 Reiller, P. E., & Descostes, M., 2020. Development and application of the thermodynamic database
986 PRODATA dedicated to the monitoring of mining activities from exploration to remediation.
987 *Chemosphere*, *251*. https://doi.org/10.1016/j.chemosphere.2020.126301

988 Richter, S., Alonso-Munoz, A., Eykens, R., Jacobsson, U., Kuehn, H., Verbruggen, A., Aregbe, Y.,
989 Wellum, R., & Keegan, E., 2008. The isotopic composition of natural uranium samples –
990 Measurements using the new n(233U)/n(236U) double spike IRMM-3636. *International Journal*
991 *of Mass Spectrometry*, *269*(1–2), 145–148. https://doi.org/10.1016/j.ijms.2007.09.012

992 Riedel, T., & Kübeck, C., 2018. Uranium in groundwater – A synopsis based on a large
993 hydrogeochemical data set. *Water Research*, *129*, 29–38.
994 https://doi.org/10.1016/j.watres.2017.11.001

995 Riotte, J., & Chabaux, F., 1999. (234U/238U) activity ratios in freshwaters as tracers of hydrological
996 processes: The Strengbach watershed (Vosges, France). *Geochimica et Cosmochimica Acta*,
997 *63*(9), 1263–1275. https://doi.org/10.1016/S0016-7037(99)00009-5

998 Rosen, M. R., Burow, K. R., & Fram, M. S., 2019. Anthropogenic and geologic causes of anomalously
999 high uranium concentrations in groundwater used for drinking water supply in the southeastern
1000 San Joaquin Valley, CA. *Journal of Hydrology*, *577*(July), 124009.
1001 https://doi.org/10.1016/j.jhydrol.2019.124009

1002 Rovan, L., Lojen, S., Zuliani, T., Kanduč, T., Petrič, M., Horvat, B., Rusjan, S., & Štrok, M., 2020.
1003 Comparison of uranium isotopes and classical geochemical tracers in Karst Aquifer of Ljubljanica
1004 River catchment (Slovenia). *Water (Switzerland)*, *12*(7). https://doi.org/10.3390/w12072064

1005 Ryu, J. S., Lee, K. S., Chang, H. W., & Cheong, C. S., 2009. Uranium isotopes as a tracer of sources of
1006 dissolved solutes in the Han River, South Korea. *Chemical Geology*, *258*(3–4), 354–361.
1007 https://doi.org/10.1016/j.chemgeo.2008.10.039

1008 Saari, H. K., Schmidt, S., Coynel, A., Huguet, S., Schäfer, J., & Blanc, G., 2007. Potential impact of
1009 former Zn ore extraction activities on dissolved uranium distribution in the Riou-Mort
1010 watershed (France). *Science of the Total Environment*, *382*, 304–310.
1011 https://doi.org/10.1016/j.scitotenv.2007.04.030

1012 Saari, H. K., Schmidt, S., Huguet, S., & Lanoux, A., 2008. Spatiotemporal variation of dissolved 238U in
1013 the Gironde fluvial-estuarine system (France). *Journal of Environmental Radioactivity*, *99*, 426–

435. https://doi.org/10.1016/j.jenvrad.2007.11.016

Salminen, R., Batista, M. J., Bidovec, M., Demetriades, A., De Vivo, B., De Vos, W., Duris, M., Gilucis, A., Gregorauskiene, V., Halamic, J., Heitzmann, P., Lima, A., Jordan, G., Klaver, G., Klein, P., Lis, J., Locutura, J., Marsina, K., Mazreku, A., O'Connor, P.J., Olsson, S.Å., Ottesen, R., Petersell, V., Plant, J.A., Reeder, S., Salpeteur, I., Sandström, H., Siewers, U., Steenfelt, A., & Tarvainen, T., 2005. *Geochemical Atlas of Europe. Part 1 - Background Information, Methodology and Maps.* Retrieved from http://weppi.gtk.fi/publ/foregsatlas/index.php

Salpeteur, I., 2010. Valeurs de référence traces dans les eaux de rivières et les sédiments, obtenues Atlas géochimique européen * (I). *Environnement, Risques & Santé*, *9*, 121–135.

Sandino, A., & Bruno, J., 1992. The solubility of (UO2)3(PO4)2 · 4H2O(s) and the formation of U(VI) phosphate complexes: Their influence in uranium speciation in natural waters. *Geochimica et Cosmochimica Acta*, *56*(12), 4135–4145. https://doi.org/10.1016/0016-7037(92)90256-I

Smedley, P. L., & Kinniburgh, D. G., 2023. Uranium in natural waters and the environment: distribution, speciation and impact. *Applied Geochemistry*, 105534. https://doi.org/10.1016/j.apgeochem.2022.105534

Smedley, P. L., Smith, B., Abesser, C., & Lapworth, D., 2006. Uranium occurrence and behaviour in British groundwater. *British Geological Survey Groundwater Programme Commissioned Report CR/06/050N*, 48.

Snow, D. D., & Spalding, R. F., 1994. Uranium isotopes in the Platte River drainage basin of the North American High plains Region. *Applied Geochemistry*, *9*(3), 271–278. https://doi.org/10.1016/0883-2927(94)90037-X

Tsumura, A., Okamoto, R., Takaku, Y., & Yamasaki, S., 1995. Direct Determination of Uranium in Rainwater by High Resolution ICP-MS with an Ultrasonic Nebulizer. *Radioisotopes*, *44*(2), 85–92. https://doi.org/10.3769/radioisotopes.44.85

Uralbekov, B., Burkitbayev, M., Satybaldiyev, B., Matveyeva, I., Tuzova, T., & Snow, D., 2014. Spatial and temporal variability of 234U/238U activity ratios in the Shu River, Central Asia. *Environmental Earth Sciences*, *72*(9), 3635–3642. https://doi.org/10.1007/s12665-014-3274-x

Van Berk, W., & Fu, Y., 2017. Redox Roll-Front Mobilization of Geogenic Uranium by Nitrate Input into Aquifers: Risks for Groundwater Resources. *Environmental Science and Technology*, *51*(1), 337–345. https://doi.org/10.1021/acs.est.6b01569

Verley, F., Brunson, F., Verjus, P., & Cholez, M., 2003. *Nappe de Beauce - Piézométrie hautes eaux 2002*.

Wang, X., Shi, Z., Kinniburgh, D. G., Zhao, L., Ni, S., Wang, R., … Zhu, B., 2019. Effect of thermodynamic database selection on the estimated aqueous uranium speciation. *Journal of Geochemical Exploration*, *204*(May), 33–42. https://doi.org/10.1016/j.gexplo.2019.05.001

Wang, Y., Frutschi, M., Suvorova, E., Phrommavanh, V., Descostes, M., Osman, A. A. A., Geipel, G., & Bernier-Latmani, R. (2013). Mobile uranium(IV)-bearing colloids in a mining-impacted wetland. *Nature Communications*, *4*(May), 1–9. https://doi.org/10.1038/ncomms3942

Wendland, F., Blum, A., Coetsiers, M., Gorova, R., Griffioen, J., Grima, J., Hinsby, K., Kunkel, R., Marandi, A., Melo, T., Panagopoulos, A., Pauwels, H., Ruisi, M., Traversa, P., Vermooten, J. S. A., & Walraevens, K., 2008. European aquifer typology: A practical framework for an overview of major groundwater composition at European scale. *Environmental Geology*, *55*(1), 77–85. https://doi.org/10.1007/s00254-007-0966-5

Windom, H., Smith, R., Niencheski, F., & Alexander, C., 2000. Uranium in rivers and estuaries of globally diverse, smaller watersheds. *Marine Chemistry*, *68*, 307–321. https://doi.org/10.1016/S0304-4203(99)00086-9

Wu, W. M., Carley, J., Green, S. J., Luo, J., Kelly, S. D., Van Nostrand, J., Lowe, K., Mehlhorn, T., Carroll, S., Boonchayanant, B., Löffler, F. E., Watson, D., Kemner, K. M., Zhou, J., Kitanidis, P. K., Kostka, J. E., Jardine, P. M., & Criddle, C. S., 2010. Effects of nitrate on the stability of uranium in a bioreduced region of the subsurface. *Environmental Science and Technology*, *44*(13), 5104–5111. https://doi.org/10.1021/es1000837

Wu, Y., Wang, Y., & Guo, W., 2019. Behavior and fate of geogenic uranium in a shallow groundwater system. *Journal of Contaminant Hydrology*, *222*(January), 41–55. https://doi.org/10.1016/j.jconhyd.2019.02.009

Zebracki, M., Cagnat, X., Gairoard, S., Cariou, N., Eyrolle-Boyer, F., Boulet, B., & Antonelli, C., 2017. U isotopes distribution in the Lower Rhone River and its implication on radionuclides disequilibrium within the decay series. *Journal of Environmental Radioactivity*, *178–179*. https://doi.org/10.1016/j.jenvrad.2017.09.004

Zhang, Y., Slomp, C. P., Peter, H., Bostick, B., Passier, H. F., Böttcher, M. E., Omoregie, E. O., Lloyd, J. R., Polya, D. A., & Cappellen, P. V., 2012. Isotopic and microbiological signatures of pyrite-driven denitrification in a sandy aquifer. *Chemical Geology*, *300–301*, 123–132. https://doi.org/10.1016/j.chemgeo.2012.01.024

Figures

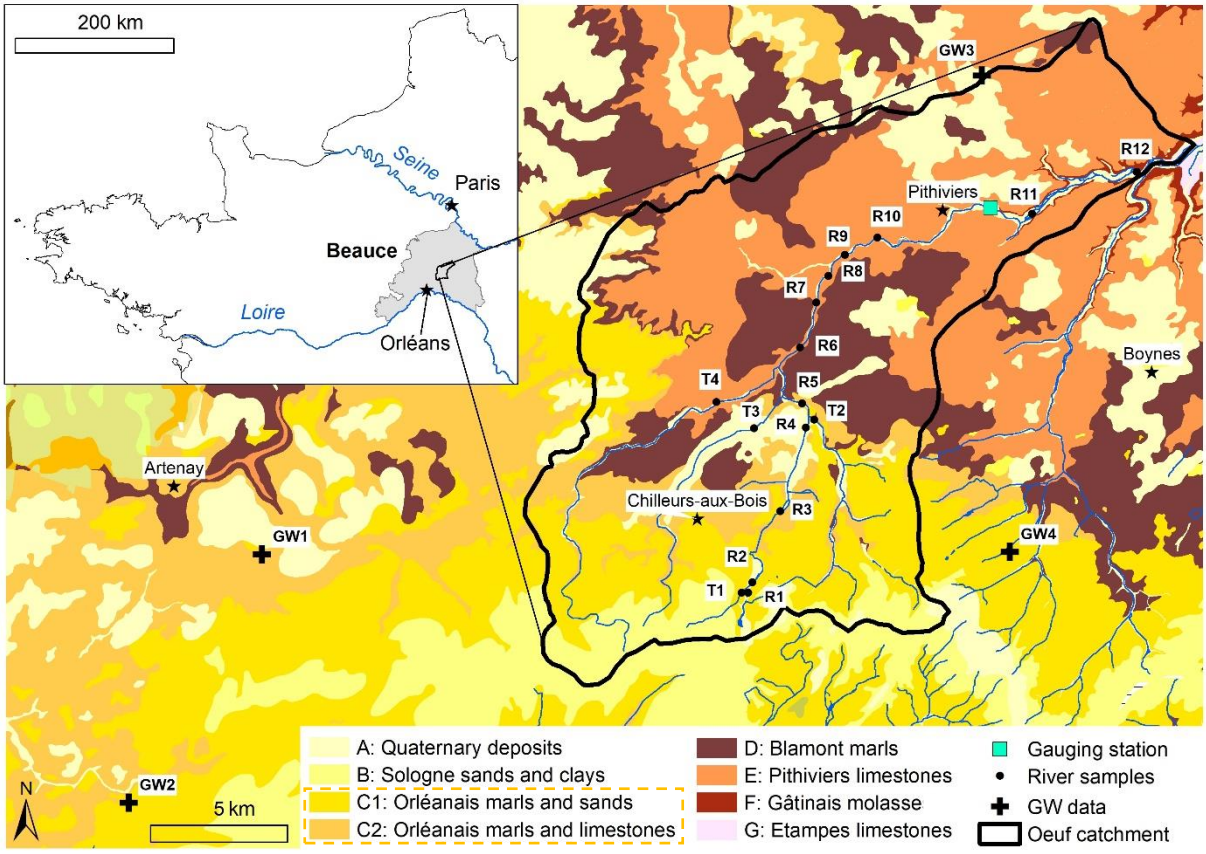

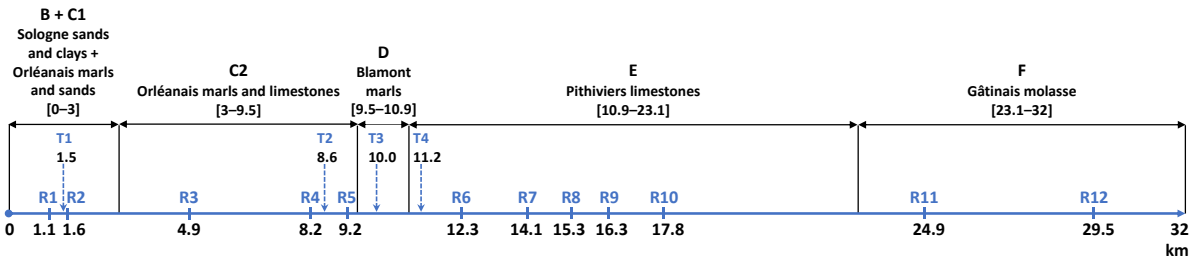

Figure 1 : Maps of the study area with the sampling sites of surface water and groundwater, and the geological formations (using ArcGis, data available from https://infoterre.brgm.fr/). Below is given the longitudinal profile of the Œuf river.

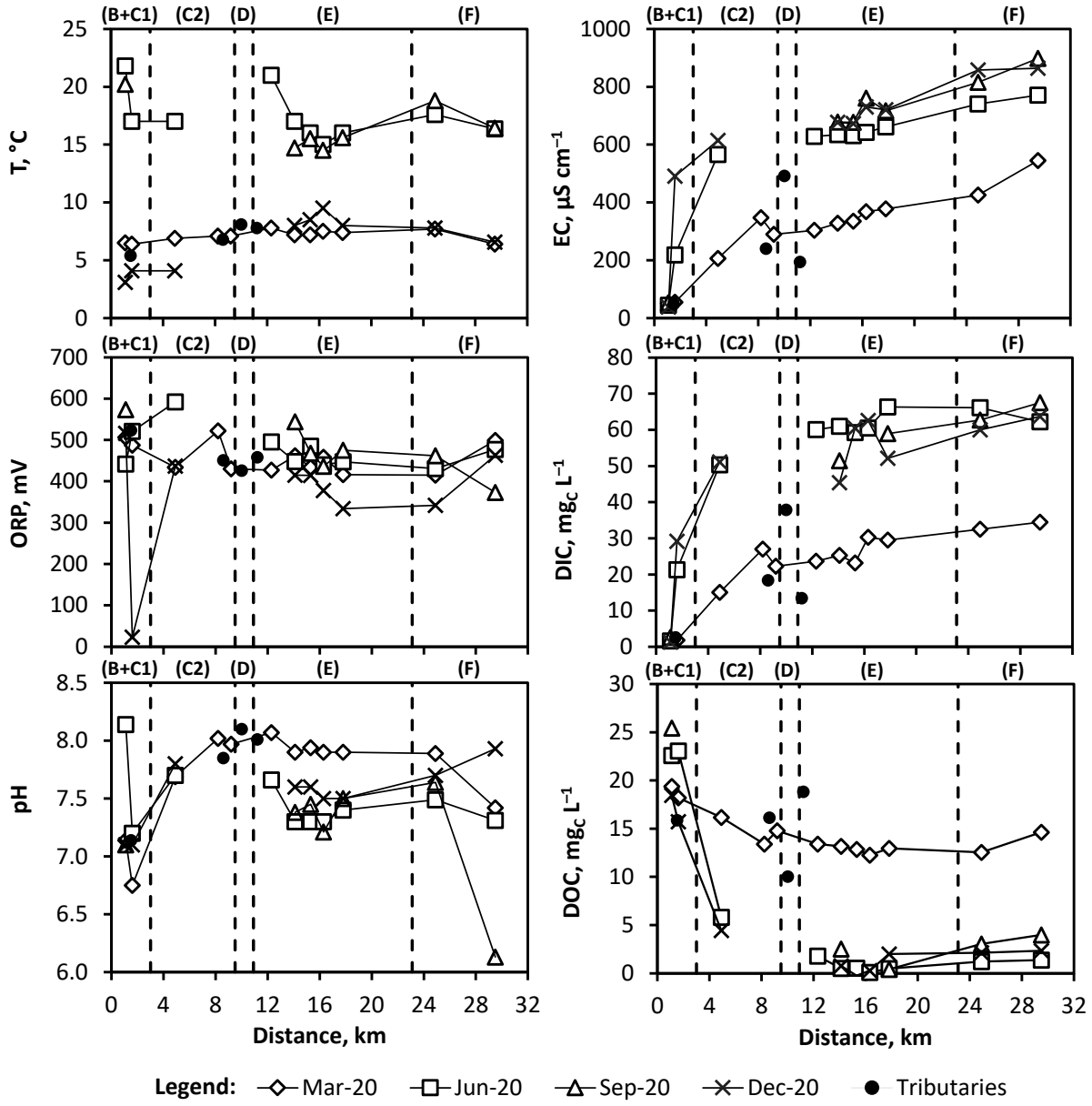

Figure 2 : Longitudinal and seasonal variations of the physical and physico-chemical parameters and the dissolved carbon concentration in the Œuf river and tributaries. The river zones where outcrop the geological formations are delineated, corresponding to (upstream to downstream): Sologne sands and clays followed by Orléanais marls and sands C1 (B+C1; 0 – 3 km), Orléanais marls and limestones (C2; 3 – 9.5 km), Blamont marls (D; 9.5 – 10.9 km), Pithiviers limestones (E; 10.9 – 23.1 km) and Gâtinais molasse (F; 23.1 – 32 km).

1091

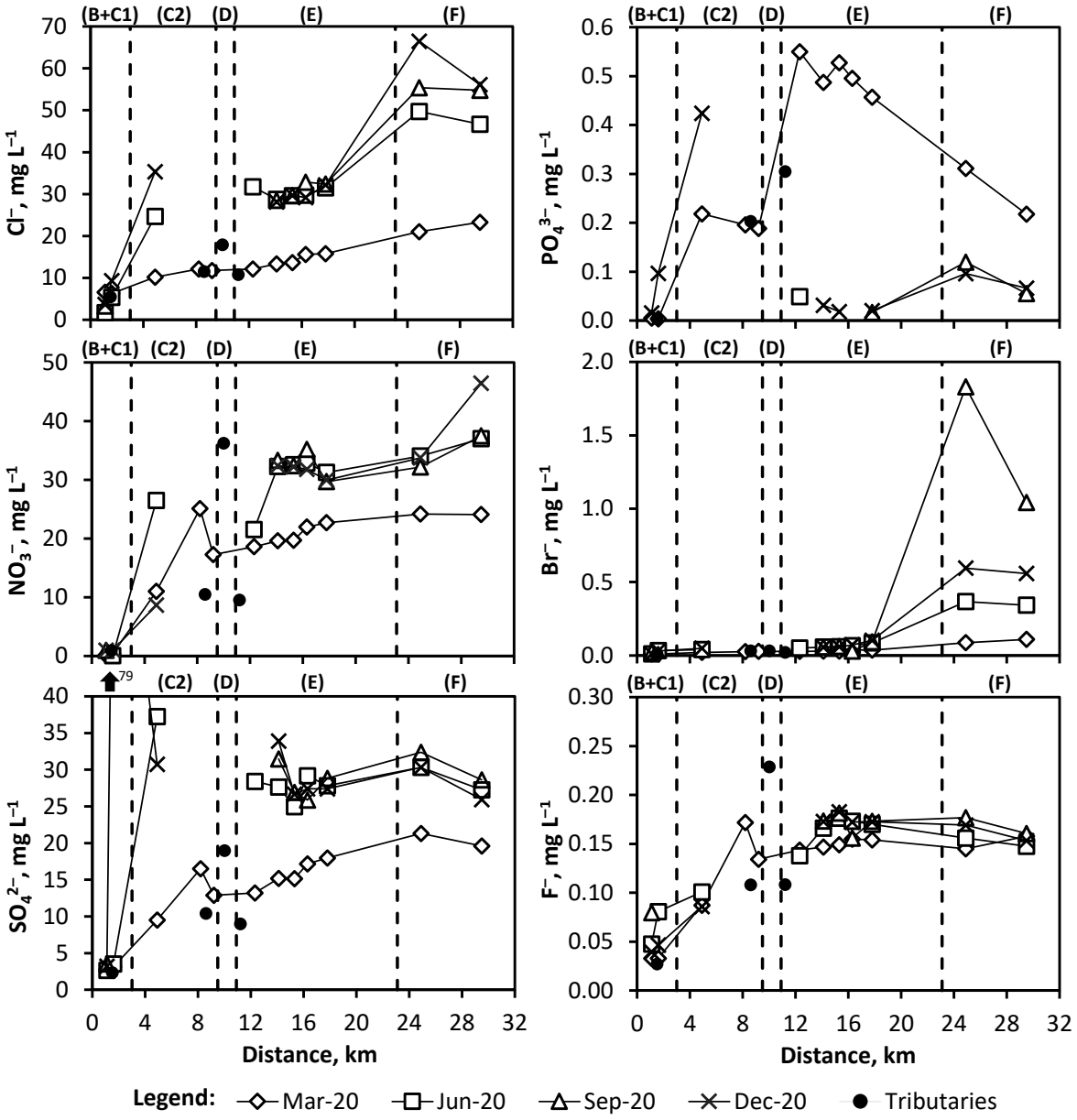

1092

1093 *Figure 3 : Longitudinal and seasonal variations of anion concentrations in the Œuf river and tributaries. The river zones*
1094 *where outcrop the geological formations are delineated, corresponding to (upstream to downstream): Sologne sands and*
1095 *clays followed by Orléanais marls and sands C1 (B+C1; 0 – 3 km), Orléanais marls and limestones (C2; 3 – 9.5 km), Blamont*
1096 *marls (D; 9.5 – 10.9 km), Pithiviers limestones (E; 10.9 – 23.1 km) and Gâtinais molasse (F; 23.1 – 32 km).*

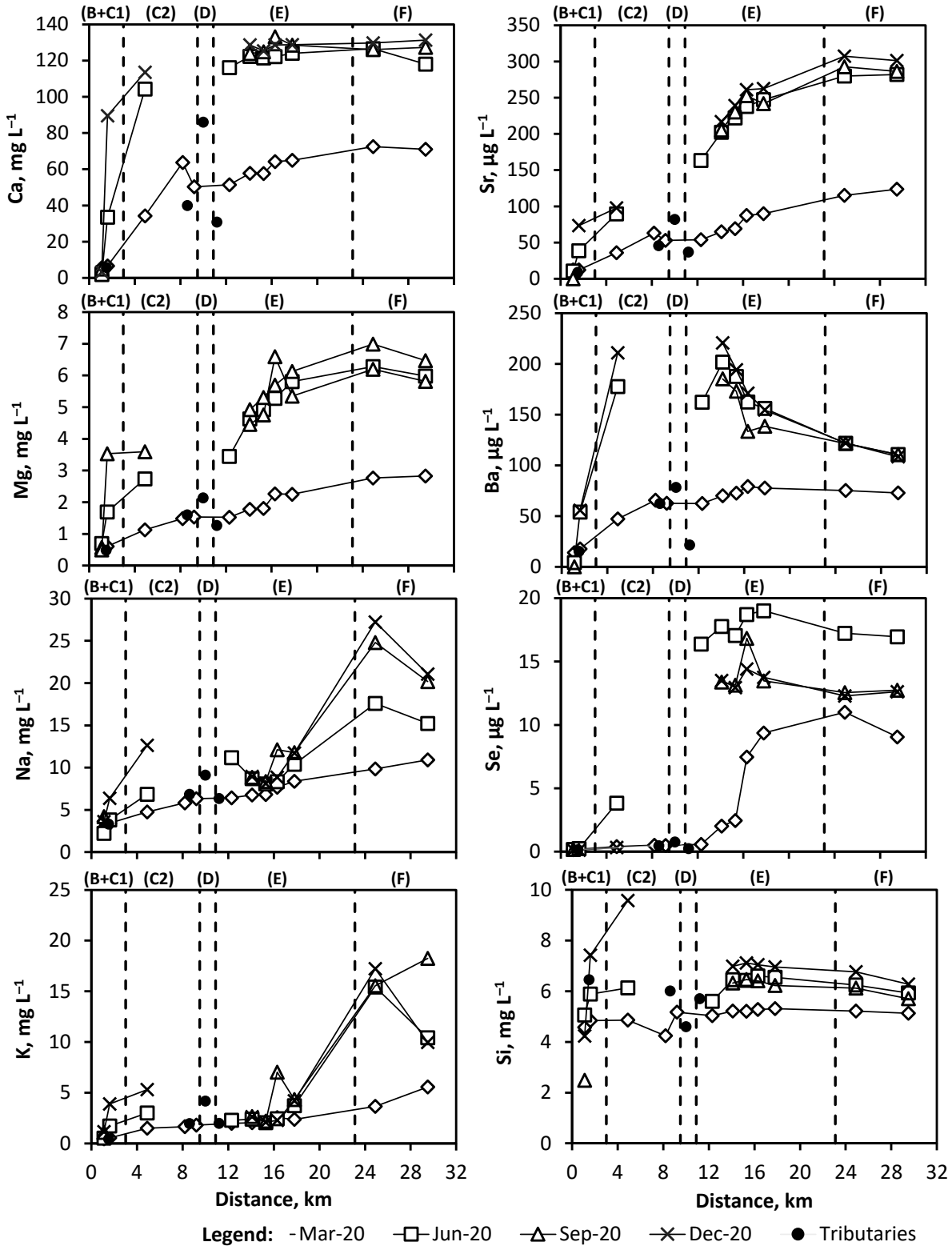

Figure 4 : Longitudinal and seasonal variations of the chemical element concentrations in the Œuf river and tributaries. The river zones where outcrop the geological formations are delineated, corresponding to (upstream to downstream): Sologne sands and clays followed by Orléanais marls and sands C1 (B+C1; 0 – 3 km), Orléanais marls and limestones (C2; 3 – 9.5 km), Blamont marls (D; 9.5 – 10.9 km), Pithiviers limestones (E; 10.9 – 23.1 km) and Gâtinais molasse (F; 23.1 – 32 km).

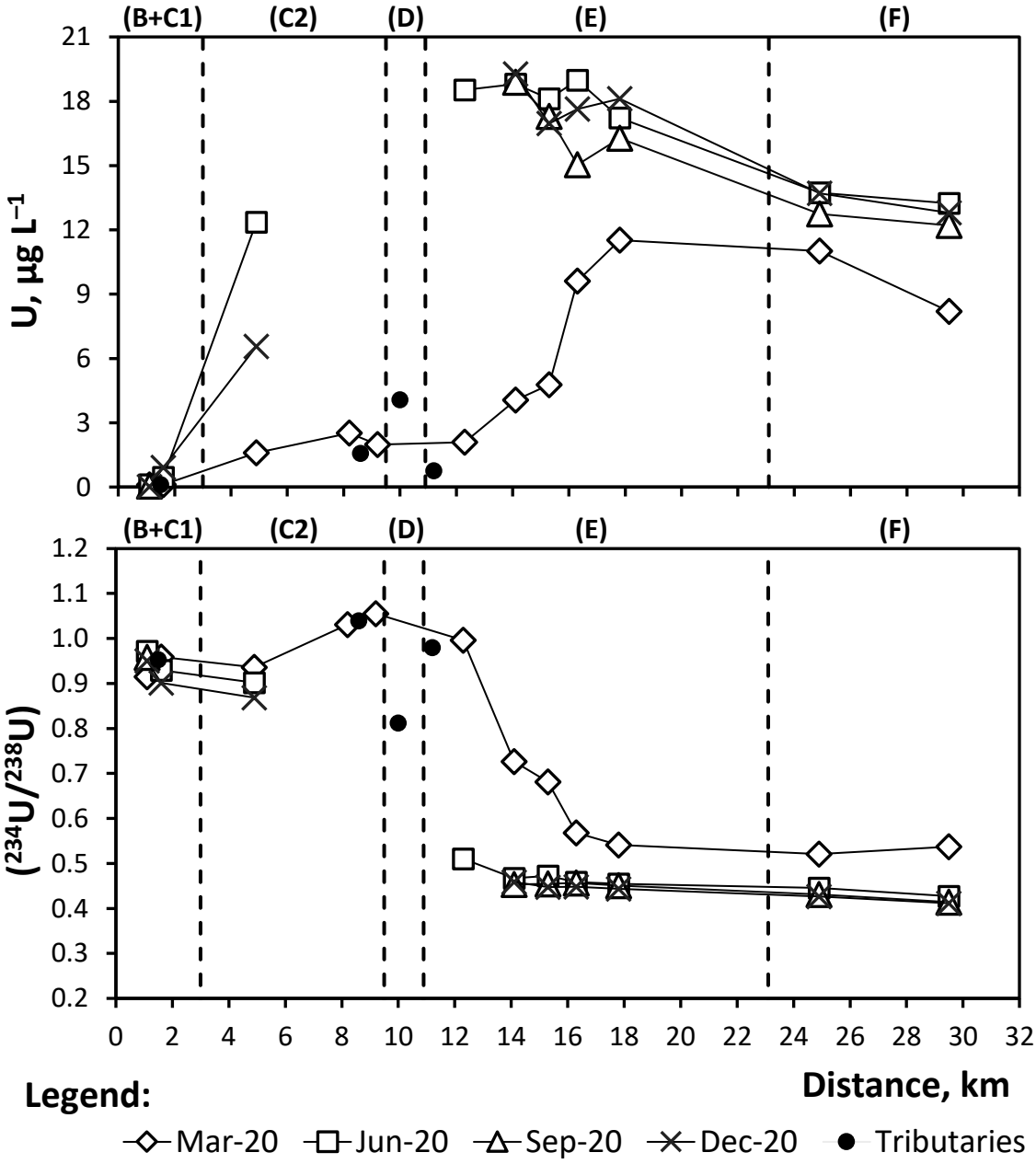

Figure 5 : Longitudinal and seasonal variations of U concentration and ($^{234}U/^{238}U$) in the Œuf river and tributaries. The river zones where outcrop the geological formations are delineated, corresponding to (upstream to downstream): Sologne sands and clays followed by Orléanais marls and sands C1 (B+C1; 0 – 3 km), Orléanais marls and limestones (C2; 3 – 9.5 km), Blamont marls (D; 9.5 – 10.9 km), Pithiviers limestones (E; 10.9 – 23.1 km) and Gâtinais molasse (F; 23.1 – 32 km).

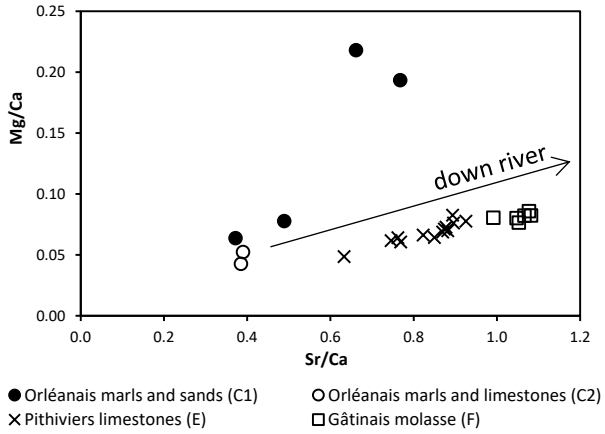

1109

1110 *Figure 6 : Plot of Mg/Ca versus Sr/Ca molar ratios in the Œuf river in LWS. Stream data are grouped according to the outcrop*
1111 *geology zone.*

1112

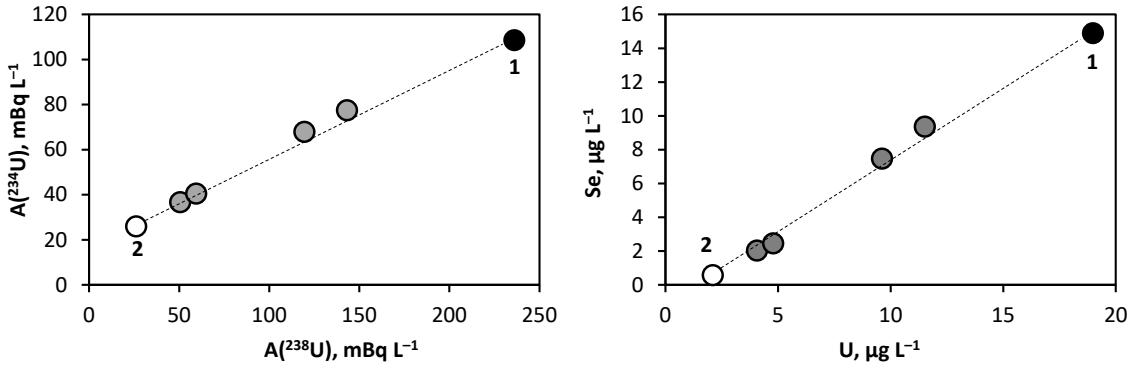

1113

1114 *Figure 7 : On the left, plot of ^{234}U versus ^{238}U activities; on the right, plot of Se versus U concentrations. Water component 1*
1115 *corresponds to the groundwater supply and water component 2 to the stream water coming from upstream.*

1116

Tables

Table 1 : Characteristics of the two water components and calculation of the mixing water volume in the Œuf river stretch R7 – R10 (14.1 – 17.8 km) in high water season (04/03/2020).

				23/06/20	21/09/20	10/12/20	Mean value
Characteristics of the water components 1 and 2	**1 = water coming from the ground**	**^{234}U, mBq L^{-1}**	R7	109	106	110	**109**
		^{238}U, mBq L^{-1}		234	235	240	**236**
		U, µg L^{-1}		18.8	18.9	19.3	**19.0**
		Se, µg L^{-1}		17.8	13.4	13.5	**14.9**
				04/03/20			
	2 = water coming from upstream	**^{234}U, mBq L^{-1}**	R6	**26.0**			
		^{238}U, mBq L^{-1}		**26.1**			
		U, µg L^{-1}		**2.1**			
		Se, µg L^{-1}		**0.6**			

			R7	R8	R9	R10
High water season (04/03/2020)	Mix 1 + 2	^{234}U, mBq L^{-1}	36.7	40.5	67.9	77.5
		^{238}U, mBq L^{-1}	50.5	59.4	120	143
		U, µg L^{-1}	4.1	4.8	9.6	11.5
		Se, µg L^{-1}	2.0	2.5	7.5	9.4

			R7	**R8**	**R9**	**R10**
			14.1 km	**15.3 km**	**16.3 km**	**17.8 km**
% Water volume	**% 1 to 2**	^{234}U	13	18	51	62
		^{238}U	12	16	44	56
		U	12	16	44	56
		Se	10	13	48	61
		Mean value	**12**	**16**	**47**	**59**
		±	1	2	3	4

Supplementary information – Figures

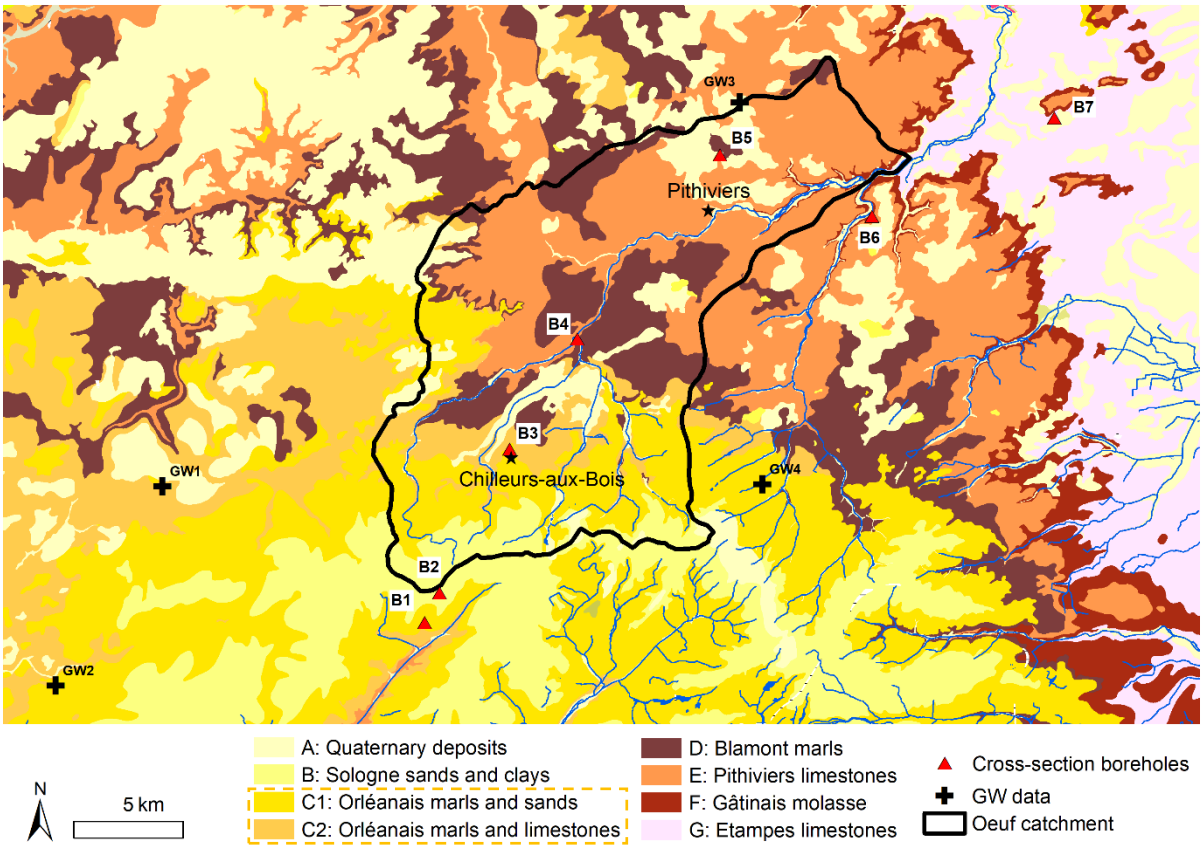

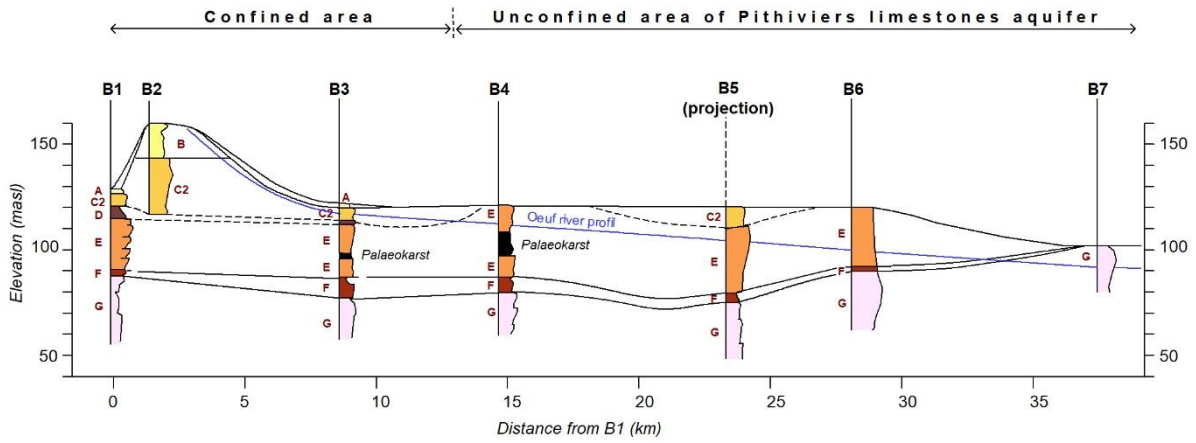

Suppl. Inf. Figure 1 : Geological map (top) and cross-section (bottom) of the Œuf river ground catchment (the figures were prepared using ArcGis and MapInfo). On the cross-section (bottom) are only reported the geological formations that outcrop in the Œuf river catchment. In the boreholes B3 and B4, sands and clays are described in the cuttings inside the Pithiviers formation and referred as palaeokarst. These deposits correspond to karst filling by materials coming from rivers flowing during the Holocene (Lorain, 1973). *The national codes of the boreholes B1 to B7 are (https://infoterre.brgm.fr/): BSS001ABMF (B1), BSS001ABSB (B2), BSS000YDWS (B3), BSS000YFBV (B4), BSS000YEMU (B5), BSS000YETY (B6) and BSS000YEXV (B7).*

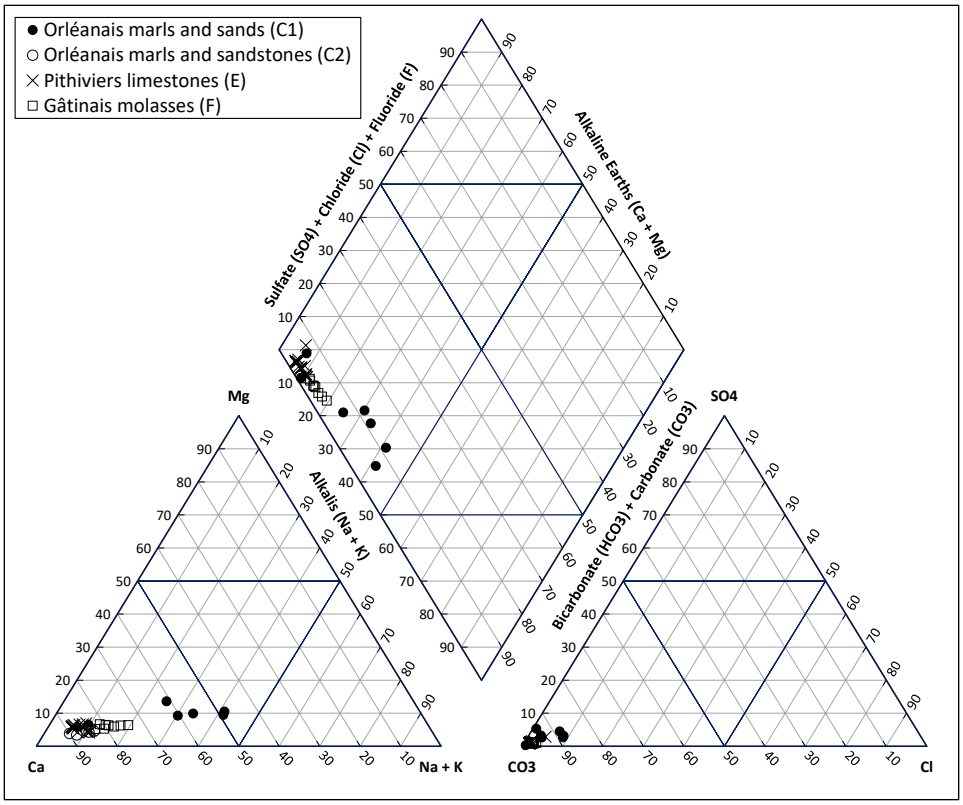

Suppl. Inf. Figure 2 : Piper diagram. Carbonate and bicarbonate correspond to the total dissolved inorganic carbon measured in the water samples.

Supplementary information – Tables

Suppl. Inf. Table 1 : Physical and physico-chemical parameters and dissolved carbon concentration measured in the Œuf river and its tributaries. Carbon results are missing for R8 and R9 in September 2020 ("Not Determined"), as samples were lost during the step sample preparation.

Sampling site	Distance km	Geology	Lat.	Long.	Date	T °C	±	pH	±	ORP mV	±	EC µS cm^{-1}	±	TC mg_C L^{-1}	±	DIC	±	DOC	±
R1	1.1	C1	48.0357	2.1307	**04/03/20**	6.5	0.1	7.1	0.1	506	5	51.3	0.5	21.3	0.1	1.9	0.2	19.4	0.2
			48.0357	2.1307	**23/06/20**	21.8	0.2	8.1	0.1	442	4	45.1	0.5	24.2	0.3	1.6	0.2	22.6	0.4
			48.0357	2.1307	**21/09/20**	20.2	0.2	7.1	0.1	573	6	53.0	0.5	28.0	0.4	2.6	0.6	25.4	0.8
			48.0357	2.1307	**10/12/20**	3.10	0.03	7.1	0.1	516	5	39.0	0.4	19.8	0.9	1.3	0.4	18	1
R2	1.6	C1	48.0357	2.1307	**04/03/20**	6.4	0.1	6.8	0.1	487	5	55.2	0.6	20.0	0.1	1.8	0.1	18.2	0.1
			48.0357	2.1307	**23/06/20**	17.0	0.2	7.2	0.1	521	5	219	2	44.4	0.5	21.3	0.6	23.1	0.8
			48.0357	2.1307	**10/12/20**	4.10	0.04	7.1	0.1	23.0	0.2	491	5	45	1	29	1	16	2
R3	4.9	C2	48.0553	2.1736	**04/03/20**	6.9	0.1	7.7	0.1	434	4	206	2	31.2	0.2	15.0	0.3	16.2	0.4
			48.0553	2.1736	**23/06/20**	17.0	0.2	7.7	0.1	592	6	566	6	56.1	0.1	50	1	5.8	0.9
			48.0553	2.1736	**10/12/20**	4.10	0.04	7.8	0.1	437	4	614	6	56	1	51	2	4	3
R4	8.2	C2	48.1020	2.1889	**04/03/20**	7.1	0.1	8.0	0.1	522	5	347	3	40.4	0.1	27.0	0.4	13.4	0.4
R5	9.2	C2	48.1044	2.1931	**04/03/20**	7.1	0.1	8.0	0.1	430	4	290	3	37.0	0.2	22.3	0.2	14.8	0.3
R6	12.3	E	48.1282	2.1862	**04/03/20**	7.8	0.1	8.1	0.1	427	4	304	3	37.1	0.1	24	1	13	1
			48.1282	2.1862	**23/06/20**	21.0	0.2	7.7	0.1	495	5	628	6	61.9	0.3	60	1	2	1
R7	14.1	E	48.1429	2.1942	**04/03/20**	7.2	0.1	7.9	0.1	462	5	328	3	38.4	0.2	25.3	0.7	13.2	0.8
			48.1429	2.1942	**23/06/20**	17.0	0.2	7.3	0.1	448	4	634	6	61.5	0.3	61	1		<1.4
			48.1429	2.1942	**21/09/20**	14.7	0.1	7.4	0.1	544	5	678	7	53.9	0.7	51	2	3	2
			48.1429	2.1942	**10/12/20**	8.0	0.1	7.6	0.1	415	4	677	7	46	1	45	2		<2.3
R8	15.3	E	48.1517	2.2001	**04/03/20**	7.2	0.1	7.9	0.1	434	4	335	3	36.0	0.1	23.1	0.2	12.9	0.2
			48.1517	2.2001	**23/06/20**	16.0	0.2	7.3	0.1	485	5	631	6	59.8	0.4	59	1		<1.1
			48.1517	2.2001	**21/09/20**	15.5	0.2	7.5	0.1	468	5	677	7	19.9	0.4	ND		ND	
			48.1517	2.2001	**10/12/20**	8.5	0.1	7.6	0.1	414	4	673	7	60	2	60	2		<2.8
R9	16.3	E	48.1587	2.2083	**04/03/20**	7.5	0.1	7.9	0.1	458	5	368	4	42.5	0.2	30.3	0.8	12.3	0.8
			48.1587	2.2083	**23/06/20**	15.0	0.2	7.3	0.1	440	4	642	6	60.6	0.4	61	1		<1.2
			48.1587	2.2083	**21/09/20**	14.5	0.1	7.2	0.1	436	4	760	8	39.7	0.5	ND		ND	
			48.1587	2.2083	**10/12/20**	9.5	0.1	7.5	0.1	378	4	730	7	63	2	63	3		<3.0
R10	17.8	E	48.1643	2.2243	**04/03/20**	7.4	0.1	7.9	0.1	416	4	378	4	42.5	0.1	29.5	0.2	13.0	0.2
			48.1643	2.2243	**23/06/20**	16.0	0.2	7.4	0.1	447	4	661	7	66.8	0.5	66.3	0.7	0.5	0.8
			48.1643	2.2243	**21/09/20**	15.6	0.2	7.5	0.1	475	5	717	7	59.3	0.7	58.9	0.9		<1.1
			48.1643	2.2243	**10/12/20**	8.0	0.1	7.5	0.1	334	3	720	7	54	1	52	2		<2.5
R11	24.9	F	48.1722	2.3003	**04/03/20**	7.7	0.1	7.9	0.1	415	4	426	4	45.1	0.1	32.5	0.1	12.5	0.2
			48.1722	2.3003	**23/06/20**	17.6	0.2	7.5	0.1	431	4	740	7	67.31	0.02	66.1	0.9	1.2	0.9
			48.1722	2.3003	**21/09/20**	18.8	0.2	7.6	0.1	462	5	815	8	65.8	0.8	63	1	3	1
			48.1722	2.3003	**10/12/20**	7.8	0.1	7.7	0.1	342	3	858	9	62	2	60	2		<2.9
R12	29.5	F	48.1860	2.3519	**04/03/20**	6.4	0.1	7.4	0.1	499	5	545	5	49.1	0.2	34.4	0.3	14.6	0.4
			48.1860	2.3519	**23/06/20**	16.4	0.2	7.3	0.1	477	5	771	8	63.6	0.2	62.2	0.7	1.4	0.7
			48.1860	2.3519	**21/09/20**	16.4	0.2	6.1	0.1	373	4	898	9	71.5	0.8	68	1	4	1
			48.1860	2.3519	**10/12/20**	6.6	0.1	7.9	0.1	463	5	864	9	66	2	64	4		<4.0
T1	1.5	C1	48.0357	2.1307	**04/03/20**	5.4	0.1	7.1	0.1	523	5	49.1	0.5	18.44	0.05	2.6	0.1	15.9	0.1
T2	8.6	C1	48.1044	2.1934	**04/03/20**	6.8	0.1	7.9	0.1	451	5	240	2	34.5	0.1	18.4	0.2	16.1	0.2
T3	10.0	A	48.1013	2.1636	**04/03/20**	8.1	0.1	8.1	0.1	426	4	492	5	47.9	0.2	37.9	0.3	10.0	0.3
T4	11.2	E	48.1101	2.1452	**04/03/20**	7.8	0.1	8.0	0.1	458	5	194	2	32.28	0.04	13.4	0.1	18.8	0.1

1143 *Suppl. Inf. Table 2 : Anion concentration measured in the Œuf river and its tributaries.*

Sampling site	Distance km	Geology	Lat.	Long.	Date	F^-	±	Cl^-	±	Br^-	±	NO_3^-	±	PO_4^{3-}	±	SO_4^{2-}	±
						mg L^{-1}											
R1	1.1	**C1**	48.0357	2.1307	**04/03/20**	0.0330	0.0005	6.58	0.03	0.0103	0.0001	0.126	0.001	0.0057	0.0004	2.82	0.03
			48.0357	2.1307	**23/06/20**	0.048	0.005	1.74	0.04		<0.01		<0.01		<0.01	2.7	0.2
			48.0357	2.1307	**21/09/20**	0.080	0.006	3.3	0.4	0.022	0.002	0.9	0.4		<0.01	3.5	0.4
			48.0357	2.1307	**10/12/20**	0.040	0.004	3.6	0.4	0.009	0.002	0.9	0.4	0.016	0.003	3.2	0.5
R2	1.6	**C1**	48.0357	2.1307	**04/03/20**	0.0330	0.0005	6.32	0.03	0.0103	0.0001	0.39	0.03	0.0041	0.0004	3.1	0.1
			48.0357	2.1307	**23/06/20**	0.081	0.006	5.364	0.004	0.032	0.005	0.040	0.004		<0.01	3.5	0.1
			48.0357	2.1307	**10/12/20**	0.047	0.004	9.4	0.5	0.032	0.002	1.0	0.4	0.097	0.005	79	4
R3	4.9	**C2**	48.0553	2.1736	**04/03/20**	0.087	0.002	10.21	0.02	0.020	0.001	10.97	0.02	0.219	0.003	9.5	0.1
			48.0553	2.1736	**23/06/20**	0.10	0.01	24.68	0.06	0.04	0.01	26.48	0.04	0.62	0.04	37	2
			48.0553	2.1736	**10/12/20**	0.086	0.004	35	2	0.049	0.003	8.6	0.5	0.42	0.03	31	2
R4	8.2	**C2**	48.1020	2.1889	**04/03/20**	0.172	0.002	12.12	0.02	0.025	0.001	25.1	0.3	0.196	0.003	16.5	0.1
R5	9.2	**C2**	48.1044	2.1931	**04/03/20**	0.134	0.002	11.80	0.02	0.028	0.001	17.24	0.02	0.189	0.004	12.9	0.2
R6	12.3	**E**	48.1282	2.1862	**04/03/20**	0.144	0.002	12.15	0.08	0.027	0.001	18.60	0.02	0.55	0.03	13.2	0.1
			48.1282	2.1862	**23/06/20**	0.14	0.01	31.76	0.04	0.05	0.01	21.50	0.04	0.05	0.04	28.4	0.2
R7	14.1	**E**	48.1429	2.1942	**04/03/20**	0.147	0.002	13.37	0.02	0.029	0.001	19.61	0.02	0.49	0.03	15.2	0.2
			48.1429	2.1942	**23/06/20**	0.17	0.01	28.74	0.04	0.06	0.01	32.28	0.05		<0.01	27.6	0.2
			48.1429	2.1942	**21/09/20**	0.173	0.009	28	1	0.057	0.003	33.3	1.8		<0.01	31	2
			48.1429	2.1942	**10/12/20**	0.173	0.009	28	1	0.055	0.003	32.4	1.7	0.032	0.003	34	2
R8	15.3	**E**	48.1517	2.2001	**04/03/20**	0.149	0.002	13.63	0.09	0.029	0.001	19.71	0.02	0.53	0.03	15.1	0.1
			48.1517	2.2001	**23/06/20**	0.18	0.01	29.64	0.04	0.06	0.01	32.55	0.04		<0.01	25.0	0.2
			48.1517	2.2001	**21/09/20**	0.182	0.009	30	2	0.060	0.003	32.4	1.7		<0.01	27	1
			48.1517	2.2001	**10/12/20**	0.183	0.009	30	2	0.059	0.003	32.2	1.7	0.019	0.003	27	1
R9	16.3	**E**	48.1587	2.2083	**04/03/20**	0.155	0.002	15.64	0.02	0.037	0.001	21.97	0.02	0.50	0.03	17.2	0.2
			48.1587	2.2083	**23/06/20**	0.17	0.01	29.73	0.04	0.07	0.01	32.84	0.04		<0.01	29.2	0.4
			48.1587	2.2083	**21/09/20**	0.156	0.008	33	2	0.029	0.002	35.2	1.8		<0.01	26	1
			48.1587	2.2083	**10/12/20**	0.172	0.008	29	1	0.070	0.004	31.8	1.6		<0.015	27	1
R10	17.8	**E**	48.1643	2.2243	**04/03/20**	0.154	0.002	15.77	0.02	0.036	0.001	22.68	0.02	0.46	0.03	18.0	0.9
			48.1643	2.2243	**23/06/20**	0.17	0.01	32	2	0.08	0.01	31.27	0.04		<0.01	27.8	0.9
			48.1643	2.2243	**21/09/20**	0.173	0.009	32	2	0.092	0.005	29.7	1.6	0.017	0.001	29	2
			48.1643	2.2243	**10/12/20**	0.173	0.009	32	2	0.103	0.006	30.0	1.5	0.021	0.003	27	1
R11	24.9	**F**	48.1722	2.3003	**04/03/20**	0.145	0.002	21.05	0.02	0.0872	0.0005	24.2	0.3	0.311	0.005	21.3	0.2
			48.1722	2.3003	**23/06/20**	0.16	0.05	49.7	0.5	0.37	0.03	34.1	0.8		<0.01	30.3	0.5
			48.1722	2.3003	**21/09/20**	0.177	0.009	55	3	1.83	0.09	32.2	1.6	0.120	0.007	32	2
			48.1722	2.3003	**10/12/20**	0.169	0.008	66	4	0.594	0.036	33.8	1.8	0.096	0.006	30	2
R12	29.5	**F**	48.1860	2.3519	**04/03/20**	0.158	0.002	23.3	0.3	0.1098	0.0005	24.1	0.3	0.218	0.003	19.6	0.1
			48.1860	2.3519	**23/06/20**	0.148	0.047	46.7	0.4	0.34	0.02	37.0	0.8		<0.01	27	1
			48.1860	2.3519	**21/09/20**	0.161	0.009	55	3	1.04	0.05	37.5	2.0	0.055	0.003	29	2
			48.1860	2.3519	**10/12/20**	0.153	0.007	56	3	0.56	0.03	46.4	2.4	0.066	0.004	26	1
T1	1.5	**C1**	48.0357	2.1307	**04/03/20**	0.0273	0.0005	5.49	0.02	0.0102	0.0001	0.88	0.03	0.0038	0.0004	2.36	0.03
T2	8.6	**C1**	48.1044	2.1934	**04/03/20**	0.108	0.002	11.55	0.02	0.030	0.001	10.46	0.02	0.203	0.003	10.4	0.1
T3	10.0	**A**	48.1013	2.1636	**04/03/20**	0.229	0.002	17.91	0.03	0.030	0.001	36.2	0.2	5.0	0.1	19.0	0.1
T4	11.2	**E**	48.1101	2.1452	**04/03/20**	0.108	0.002	10.78	0.02	0.020	0.001	9.51	0.02	0.305	0.003	9.0	0.2

1144

1145

1146 *Suppl. Inf. Table 3 : Chemical element concentration measured in the Œuf river and its tributaries.*

Sampling site	Distance km	Geology	Lat.	Long.	Date	Si	±	Na	±	K	±	Mg	±	Ca	±
						mg L^{-1}									
R1	1.1	**C1**	48.0357	2.1307	**04/03/20**	4.6	0.1	3.631	0.005	0.45	0.03	0.60	0.05	5.7	0.2
			48.0357	2.1307	**23/06/20**	5.1	0.2	2.23	0.04	0.52	0.01	0.70	0.01	1.86	0.09
			48.0357	2.1307	**21/09/20**	2.5	0.1	4.22	0.03	1.09	0.02	0.58	0.03	4.86	0.09
			48.0357	2.1307	**10/12/20**	4.2	0.1	3.62	0.07	1.16	0.03	0.50	0.01	3.2	0.2
R2	1.6	**C1**	48.0357	2.1307	**04/03/20**	4.8	0.2	3.43	0.02	0.54	0.02	0.61	0.07	6.5	0.2
			48.0357	2.1307	**23/06/20**	5.9	0.1	3.81	0.04	1.71	0.02	1.69	0.01	33.5	0.9
			48.0357	2.1307	**10/12/20**	7.4	0.1	6.37	0.09	3.90	0.03	3.5	0.3	90	9
R3	4.9	**C2**	48.0553	2.1736	**04/03/20**	4.9	0.1	4.8	0.1	1.50	0.06	1.13	0.04	34.2	0.3
			48.0553	2.1736	**23/06/20**	6.1	0.1	6.8	0.1	3.01	0.05	2.73	0.04	104	2
			48.0553	2.1736	**10/12/20**	9.6	0.2	12.6	0.3	5.3	0.1	3.6	0.3	114	11
R4	8.2	**C2**	48.1020	2.1889	**04/03/20**	4.2	0.1	5.84	0.01	1.64	0.07	1.5	0.1	64	1
R5	9.2	**C2**	48.1044	2.1931	**04/03/20**	5.2	0.1	6.3	0.2	1.80	0.02	1.5	0.1	50	1
R6	12.3	**E**	48.1282	2.1862	**04/03/20**	5.0	0.0	6.43	0.02	1.98	0.01	1.5	0.1	51	1
			48.1282	2.1862	**23/06/20**	5.6	0.1	11.2	0.4	2.28	0.01	3.4	0.1	116.0	0.6
R7	14.1	**E**	48.1429	2.1942	**04/03/20**	5.2	0.1	6.8	0.1	2.04	0.02	1.8	0.1	58	1
			48.1429	2.1942	**23/06/20**	6.45	0.01	8.7	0.2	2.39	0.01	4.63	0.03	122	2
			48.1429	2.1942	**21/09/20**	6.3	0.1	8.9	0.1	2.65	0.02	4.5	0.2	124	3
			48.1429	2.1942	**10/12/20**	6.98	0.05	9.0	0.1	2.64	0.02	4.9	0.3	129	15
R8	15.3	**E**	48.1517	2.2001	**04/03/20**	5.2	0.1	6.83	0.03	2.07	0.03	1.8	0.1	58	1
			48.1517	2.2001	**23/06/20**	6.4	0.1	8.1	0.2	2.04	0.02	4.9	0.2	121.5	0.8
			48.1517	2.2001	**21/09/20**	6.5	0.1	8.3	0.1	2.18	0.02	4.8	0.2	125	3
			48.1517	2.2001	**10/12/20**	7.1	0.1	8.14	0.07	2.09	0.01	5.3	0.3	125	15
R9	16.3	**E**	48.1587	2.2083	**04/03/20**	5.3	0.1	7.68	0.01	2.55	0.09	2.3	0.1	64	1
			48.1587	2.2083	**23/06/20**	6.60	0.04	8.3	0.1	2.44	0.01	5.3	0.2	122	1
			48.1587	2.2083	**21/09/20**	6.4	0.1	12.1	0.1	7.03	0.09	6.6	0.1	133	1
			48.1587	2.2083	**10/12/20**	7.0	0.1	8.86	0.07	2.29	0.04	5.7	0.5	129	13
R10	17.8	**E**	48.1643	2.2243	**04/03/20**	5.3	0.1	8.4	0.2	2.36	0.03	2.3	0.1	65	1
			48.1643	2.2243	**23/06/20**	6.5	0.2	10.4	0.1	3.72	0.07	5.8	0.1	124	4
			48.1643	2.2243	**21/09/20**	6.2	0.1	11.8	0.2	4.32	0.06	5.4	0.2	129	1
			48.1643	2.2243	**10/12/20**	6.95	0.05	11.7	0.4	4.20	0.04	6.1	0.5	129	18
R11	24.9	**F**	48.1722	2.3003	**04/03/20**	5.22	0.04	9.86	0.04	3.66	0.04	2.8	0.1	72	1
			48.1722	2.3003	**23/06/20**	6.2	0.2	17.6	0.4	15.4	0.5	6.3	0.1	127	2
			48.1722	2.3003	**21/09/20**	6.1	0.1	24.8	0.4	15.5	0.1	6.2	0.1	126	3
			48.1722	2.3003	**10/12/20**	6.8	0.1	27.2	0.7	17.2	0.2	7.0	0.2	130	15
R12	29.5	**F**	48.1860	2.3519	**04/03/20**	5.1	0.1	10.93	0.03	5.56	0.09	2.8	0.1	71	1
			48.1860	2.3519	**23/06/20**	5.9	0.1	15.2	0.3	10.4	0.1	6.0	0.1	118	1
			48.1860	2.3519	**21/09/20**	5.70	0.03	20.2	0.7	18.3	0.3	5.8	0.1	127	5
			48.1860	2.3519	**10/12/20**	6.3	0.1	21.1	0.4	10.0	0.1	6.5	0.2	131	18
T1	1.5	**C1**	48.0357	2.1307	**04/03/20**	6.4	0.1	3.33	0.02	0.43	0.02	0.49	0.05	5.7	0.2
T2	8.6	**C1**	48.1044	2.1934	**04/03/20**	6.0	0.1	6.9	0.1	2.0	0.1	1.6	0.1	40	1
T3	10.0	**A**	48.1013	2.1636	**04/03/20**	4.6	0.1	9.1	0.1	4.2	0.1	2.1	0.1	86	1
T4	11.2	**E**	48.1101	2.1452	**04/03/20**	5.7	0.1	6.3	0.2	1.98	0.05	1.3	0.1	30.8	0.4

1147

1148

Suppl. Inf. Table 4 : Chemical element concentration (continued) and ($^{234}U/^{238}U$) activity ratio measured in the Œuf river and its tributaries.

Sampling site	Distance km	Geology	Lat.	Long.	Date	Sr	±	Ba	±	Fe	±	Mn	±	Se	±	U	±	AR	±
						µg L^{-1}													
R1	1.1	**C1**	48.0357	2.1307	**04/03/20**	12.3	0.3	13.9	0.5	186	1	21.7	0.2	0.18	0.02	**0.098**	0.001	**0.92**	0.02
			48.0357	2.1307	**23/06/20**	<10		<10		1011	37	11.1	0.4	0.18	0.02	**0.111**	0.001	**0.97**	0.03
			48.0357	2.1307	**21/09/20**	<10		<10		252	8	<10		0.18	0.03	**0.0517**	0.0004	**0.96**	0.03
			48.0357	2.1307	**10/12/20**	<10		<10		750	20	23.0	0.6	0.15	0.03	**0.0197**	0.0001	**0.95**	0.05
R2	1.6	**C1**	48.0357	2.1307	**04/03/20**	12.1	0.9	18	1	225	1	22.5	0.3	0.19	0.01	**0.111**	0.001	**0.96**	0.06
			48.0357	2.1307	**23/06/20**	38.7	0.2	53.8	0.3	793	23	178	3	0.26	0.02	**0.451**	0.003	**0.93**	0.02
			48.0357	2.1307	**10/12/20**	73	2	56	2	340	6	268	4	0.13	0.09	**0.914**	0.004	**0.90**	0.02
R3	4.9	**C2**	48.0553	2.1736	**04/03/20**	35.9	0.3	47	2	128	1	21.1	0.2	0.40	0.04	**1.59**	0.01	**0.94**	0.01
			48.0553	2.1736	**23/06/20**	89.4	0.3	178	1	28.7	0.9	18.5	0.4	3.8	0.1	**12.35**	0.04	**0.902**	0.002
			48.0553	2.1736	**10/12/20**	98	2	211	4	<10		15.4	0.6	0.34	0.07	**6.55**	0.04	**0.87**	0.01
R4	8.2	**C2**	48.1020	2.1889	**04/03/20**	63.1	0.4	66	1	93	1	<10		0.51	0.03	**2.52**	0.02	**1.03**	0.01
R5	9.2	**C2**	48.1044	2.1931	**04/03/20**	52.9	0.1	63	3	104.4	0.3	10.2	0.1	0.49	0.02	**1.99**	0.01	**1.06**	0.02
R6	12.3	**E**	48.1282	2.1862	**04/03/20**	54.0	0.7	62.3	0.4	105	1	<10		0.57	0.02	**2.10**	0.01	**1.00**	0.01
			48.1282	2.1862	**23/06/20**	163	1	162	2	12.9	0.9	<10		16	1	**18.53**	0.07	**0.51**	0.01
R7	14.1	**E**	48.1429	2.1942	**04/03/20**	65.0	0.4	70	1	85.4	0.5	<10		2.0	0.1	**4.06**	0.02	**0.73**	0.01
			48.1429	2.1942	**23/06/20**	202	3	202	4	8.5	0.9	<10		17.8	0.2	**18.80**	0.09	**0.47**	0.01
			48.1429	2.1942	**21/09/20**	205	5	185	5	11.7	0.4	<10		13.4	0.4	**18.89**	0.04	**0.45**	0.01
			48.1429	2.1942	**10/12/20**	217	3	221	3	<10		<10		13.5	0.4	**19.27**	0.08	**0.459**	0.004
R8	15.3	**E**	48.1517	2.2001	**04/03/20**	69.1	0.5	72.6	0.5	103.0	0.6	<10		2.5	0.1	**4.78**	0.02	**0.68**	0.01
			48.1517	2.2001	**23/06/20**	222	2	188	1	10.1	0.5	<10		17.1	0.1	**18.12**	0.06	**0.473**	0.005
			48.1517	2.2001	**21/09/20**	230	7	173	5	12	1	<10		13.1	0.3	**17.30**	0.04	**0.454**	0.005
			48.1517	2.2001	**10/12/20**	239	2	194	2	<10		<10		13.0	0.3	**17.0**	0.1	**0.45**	0.01
R9	16.3	**E**	48.1587	2.2083	**04/03/20**	87.4	0.3	79	1	88.1	0.9	<10		7.5	0.2	**9.61**	0.05	**0.57**	0.02
			48.1587	2.2083	**23/06/20**	238	1	163	1	13.1	0.2	<10		18.7	0.3	**18.98**	0.10	**0.46**	0.01
			48.1587	2.2083	**21/09/20**	253	5	133	4	12.5	0.8	<10		16.8	0.4	**15.04**	0.03	**0.46**	0.01
			48.1587	2.2083	**10/12/20**	261	4	171	6	<10		<10		14.4	0.5	**17.64**	0.07	**0.45**	0.01
R10	17.8	**E**	48.1643	2.2243	**04/03/20**	89.9	0.4	77.6	0.1	77.1	0.5	<10		9.4	0.1	**11.52**	0.06	**0.54**	0.01
			48.1643	2.2243	**23/06/20**	247	1	156	2	13	1	<10		19.0	0.2	**17.22**	0.09	**0.45**	0.01
			48.1643	2.2243	**21/09/20**	242	5	138	9	16.2	0.8	<10		13.5	0.5	**16.27**	0.04	**0.45**	0.01
			48.1643	2.2243	**10/12/20**	262	3	155	2	22	1	<10		13.8	0.4	**18.11**	0.09	**0.444**	0.005
R11	24.9	**F**	48.1722	2.3003	**04/03/20**	115.2	0.4	75	4	76.2	0.2	13.5	0.1	11.0	0.1	**11.01**	0.06	**0.52**	0.02
			48.1722	2.3003	**23/06/20**	280	4	122	3	26.3	0.6	13.9	0.2	17	2	**13.73**	0.05	**0.45**	0.01
			48.1722	2.3003	**21/09/20**	293	6	121	3	25	1	<10		12.6	0.3	**12.74**	0.04	**0.43**	0.01
			48.1722	2.3003	**10/12/20**	307	3	122	2	49	1	18.3	0.4	12.3	0.4	**13.71**	0.09	**0.43**	0.01
R12	29.5	**F**	48.1860	2.3519	**04/03/20**	123.5	0.4	72.8	0.4	94	1	16.5	0.3	9	1	**8.20**	0.04	**0.54**	0.02
			48.1860	2.3519	**23/06/20**	282	4	111	2	26.0	0.7	<10		17.0	0.2	**13.24**	0.05	**0.43**	0.01
			48.1860	2.3519	**21/09/20**	286	4	111	1	23.7	0.2	<10		12.7	0.3	**12.21**	0.03	**0.414**	0.003
			48.1860	2.3519	**10/12/20**	301	3	108	2	41	1	<10		12.6	0.2	**12.79**	0.05	**0.41**	0.01
T1	1.5	**C1**	48.0357	2.1307	**04/03/20**	8.8	0.4	15	2	205	1	<10		0.16	0.01	**0.110**	0.001	**0.95**	0.03
T2	8.6	**C1**	48.1044	2.1934	**04/03/20**	46	1	62	3	117	1	13.8	0.3	0.48	0.02	**1.57**	0.01	**1.04**	0.02
T3	10.0	**A**	48.1013	2.1636	**04/03/20**	82	1	78	3	38.3	0.5	<10		0.78	0.04	**4.07**	0.02	**0.81**	0.01
T4	11.2	**E**	48.1101	2.1452	**04/03/20**	36.9	0.3	21	2	275.9	0.4	<10		0.26	0.02	**0.76**	0.01	**0.98**	0.04

Groundwater code	Borehole national code	BLAS unit	Dataset	σ (25°C)	ORP	Cl^-	NO_3^-	Ca	Mg	Se	U	($^{234}U/^{238}U$)
				µS cm^{-1}	mV	mg L^{-1}				µg L^{-1}		
			Period	2001 – 2020		1997 – 2020	1991 – 2020	1997 – 2020		1998 – 2020	2012 – 2018	
			n	37		35	54	13	13	38	4	4
GW1	BSS001AAZQ	Orléanais limestone formation	min	543	ND	20	21	94	4	7	10	0.37
			MAX	631		25	36	109	5	15	11	0.38
			mean	572		23	29	103	5	11	11	0.38
			Period	2005 – 2006		2001 – 2006						
			n	4	10	11	10	11	11			
GW2	BSS001AAWC	Pithiviers limestones	min	605	100	25	45	96	5		ND	
			MAX	800	268	71	54	121	6			
			mean	691	150	49	45	111	6			
			Period	2001 – 2021		1992 – 2021	1991 – 2021	1992 – 2020		1998 – 2021	2011	
			n	38		40	72	17	17	44	1	1
GW3	BSS000YEJL	Pithiviers limestones	min	503	ND	16	34	85	4.1	5	7.3	0.32
			MAX	585		28	55	102	5.3	12	7.3	0.32
			mean	554		23	44	95	5	9	7.3	0.32
			Period	2001 – 2021		1991 – 2021				2010 – 2021	2009 – 2020	
			n	47		49	34	31	31	15	6	6
GW4	BSS000YFHV	Pithiviers limestones + Etampes limestones	min	532	ND	19	0.10	95	7	2	11	0.43
			MAX	646		24	1.1	112	8.3	3	12	0.47
			mean	586		22	0.55	102	7	2	12	0.45

Suppl. Inf. Table 5 : Characteristics of the groundwater extracted from the BLAS aquifer units featured in the Œuf river catchment. Data are available from the French national web portal ADES (https://ades.eaufrance.fr/).

Suppl. Inf. Table 6 : Correlation coefficient between the analytes measured in the Œuf river.

T	pH	Eh	EC	TC	DIC	DOC	F^-	Cl^-	Br^-	NO_3^-	PO_4^{3-}	SO_4^{2-}	Si	Na	K	Mg	Ca	Sr	Ba	Fe	Mn	Se	U	AR	
1.00	-0.20	0.34	0.24	0.31	0.33	-0.28	0.18	0.24	0.29	0.34	-0.07	0.02	-0.06	0.14	0.19	0.27	0.24	0.49	0.43	0.02	-0.05	0.43	0.35	-0.27	**T**
	1.00	0.08	-0.10	-0.08	-0.08	0.01	0.21	-0.11	-0.17	0.15	0.55	-0.10	0.02	-0.06	-0.24	-0.17	-0.06	-0.22	-0.01	-0.01	-0.42	-0.17	-0.06	0.14	**pH**
		1.00	-0.23	-0.15	-0.14	0.01	0.01	-0.12	-0.08	0.01	0.19	-0.65	-0.44	-0.18	-0.22	-0.28	-0.23	-0.10	0.10	0.004	-0.66	-0.04	-0.01	0.11	**Eh**
			1.00	**0.84**	**0.97**	**-0.91**	0.75	**0.91**	0.48	**0.87**	-0.21	0.67	0.68	0.79	0.66	**0.96**	**0.98**	**0.94**	0.71	-0.64	0.01	**0.81**	**0.83**	**-0.84**	**EC**
				1.00	**0.98**	**-0.87**	0.62	0.79	0.47	0.70	-0.11	0.56	0.56	0.70	0.60	0.79	**0.81**	0.74	0.57	-0.51	0.07	0.71	0.70	-0.68	**TC**
					1.00	**-0.94**	0.75	**0.86**	0.42	**0.85**	-0.15	0.61	0.67	0.71	0.57	**0.93**	**0.97**	**0.92**	0.78	-0.63	-0.05	**0.86**	**0.88**	**-0.82**	**DIC**
						1.00	-0.65	**-0.88**	-0.42	**-0.82**	-0.17	-0.54	-0.58	-0.76	-0.62	**-0.87**	**-0.94**	**-0.86**	**-0.84**	0.67	0.28	**-0.80**	**-0.88**	0.72	**DOC**
							1.00	0.61	0.26	**0.88**	0.09	0.30	0.32	0.51	0.33	0.69	0.76	0.69	0.55	-0.71	-0.30	0.75	0.78	-0.77	**F^-**
								1.00	0.68	0.79	-0.26	0.47	0.53	**0.95**	**0.85**	**0.89**	**0.83**	**0.89**	0.49	-0.56	-0.26	0.72	0.68	-0.76	**Cl^-**
									1.00	0.38	-0.23	0.20	0.10	0.79	**0.81**	0.47	0.34	0.51	0.02	-0.21	-0.19	0.26	0.17	-0.37	**Br^-**
										1.00	-0.04	0.36	0.38	0.64	0.50	**0.83**	**0.85**	**0.86**	0.59	-0.74	-0.46	**0.83**	**0.83**	**-0.83**	**NO_3^-**
											1.00	-0.08	-0.06	-0.23	-0.22	-0.37	-0.17	-0.48	-0.09	-0.23	-0.20	-0.36	-0.21	0.26	**PO_4^{3-}**
												1.00	0.67	0.40	0.34	0.61	0.70	0.41	0.43	-0.40	0.56	0.41	0.48	-0.42	**SO_4^{2-}**
													1.00	0.39	0.26	0.66	0.74	0.47	0.73	-0.32	0.29	0.43	0.56	-0.45	**Si**
														1.00	**0.92**	0.77	0.67	0.75	0.25	-0.47	-0.20	0.55	0.48	-0.65	**Na**
															1.00	0.65	0.51	0.64	0.07	-0.31	-0.11	0.41	0.28	-0.49	**K**
																1.00	**0.94**	**0.98**	0.65	-0.54	0.04	**0.86**	**0.82**	**-0.86**	**Mg**
																	1.00	**0.91**	**0.83**	-0.67	0.05	**0.83**	**0.89**	**-0.82**	**Ca**
																		1.00	0.63	-0.53	-0.22	**0.87**	**0.82**	**-0.88**	**Sr**
																			1.00	-0.54	-0.25	0.66	**0.85**	-0.58	**Ba**
																				1.00	0.29	-0.58	-0.64	0.58	**Fe**
																					1.00	-0.28	-0.33	0.20	**Mn**
																						1.00	**0.93**	**-0.93**	**Se**
																							1.00	**-0.89**	**U**
																								1.00	**AR**

Suppl. Inf. Table 7 : Modelled speciation of U aqueous species in the Œuf river.

Sampling site	Distance km	Sampling date	U	U(IV)	U(VI)	$UO_2(CO_3)_2^{2-}$	$UO_2(CO_3)_4^{3-}$	$UO_2(CO_3)$	$UO_2(HPO_4)_2^{2-}$	UO_2OH^+	UO_2^{2+}	Σ (U – CO_3)	Σ (U – PO_4)	Other U(VI)
			mol L^{-1}									%		
R1	1.1	04/03/20	4.2E-10	1.9E-28	4.2E-10	2.0E-12	4.3E-14	1.9E-12	4.2E-10	3.9E-14	8.6E-15	0.9	99.0	0
R2	1.6	04/03/20	4.6E-10	1.4E-25	4.6E-10	1.3E-10	1.1E-12	3.2E-10	0.0E+00	7.0E-12	3.8E-12	97.6	0	2.3
R3	4.9	04/03/20	6.7E-09	2.9E-27	6.7E-09	3.0E-11	2.4E-11	8.7E-13	6.6E-09	2.5E-15	1.7E-16	0.8	99.2	0
R4	8.2	04/03/20	1.1E-08	1.4E-29	1.1E-08	6.4E-10	2.5E-09	4.6E-12	7.5E-09	8.0E-15	2.6E-16	29.6	70.4	0
R5	9.2	04/03/20	8.4E-09	1.2E-26	8.4E-09	3.4E-10	8.9E-10	3.4E-12	7.1E-09	6.9E-15	2.4E-16	14.7	85.3	0
R6	12.3	04/03/20	8.8E-09	3.4E-27	8.8E-09	8.9E-11	3.0E-10	6.5E-13	8.4E-09	1.3E-15	3.5E-17	4.4	95.6	0
R7	14.1	04/03/20	1.7E-08	4.0E-28	1.7E-08	1.2E-10	3.2E-10	1.2E-12	1.7E-08	2.3E-15	9.5E-17	2.6	97.4	0
R8	15.3	04/03/20	2.0E-08	2.7E-27	2.0E-08	1.2E-10	3.2E-10	1.2E-12	2.0E-08	2.5E-15	9.4E-17	2.2	97.8	0
R9	16.3	04/03/20	4.0E-08	9.4E-28	4.0E-08	4.3E-10	1.4E-09	3.5E-12	3.9E-08	5.5E-15	2.3E-16	4.5	95.5	0
R10	17.8	04/03/20	4.8E-08	3.3E-26	4.8E-08	5.7E-10	1.8E-09	4.9E-12	4.6E-08	7.8E-15	3.2E-16	5.0	95.0	0
R11	24.9	04/03/20	4.6E-08	1.0E-25	4.6E-08	1.4E-09	5.1E-09	1.1E-11	4.0E-08	1.6E-14	6.7E-16	14.0	86.0	0
R12	29.5	04/03/20	3.4E-08	8.7E-29	3.4E-08	3.9E-10	5.5E-10	8.6E-12	3.4E-08	1.1E-14	1.5E-15	2.8	97.2	0
R3	4.9	23/06/20	5.2E-08	2.4E-32	5.2E-08	1.4E-09	3.4E-09	7.1E-12	4.7E-08	0	0	9.3	90.7	0
R6	12.3	23/06/20	7.8E-08	2.8E-28	7.8E-08	2.1E-08	5.4E-08	7.7E-11	2.1E-09	0	0	97.3	2.7	0
R10	17.8	21/09/20	6.8E-08	3.8E-27	6.8E-08	2.1E-08	4.7E-08	1.5E-10	8.4E-10	0	0	98.8	1.2	0
R11	24.9	21/09/20	5.4E-08	2.6E-27	5.4E-08	1.2E-08	3.3E-08	4.8E-11	8.9E-09	0	0	83.4	16.6	0
R12	29.5	21/09/20	5.1E-08	6.8E-23	5.1E-08	8.0E-09	9.0E-10	1.1E-09	4.1E-08	0	0	19.4	80.6	0
R1	1.1	10/12/20	8.3E-11	7.6E-30	8.3E-11	4.8E-14	7.9E-16	8.1E-14	8.2E-11	0	0	0.2	99.8	0
R2	1.6	10/12/20	3.8E-09	7.3E-13	3.8E-09	5.3E-11	3.9E-11	3.1E-12	3.7E-09	0	0	2.5	97.5	0
R3	4.9	10/12/20	2.8E-08	5.1E-27	2.8E-08	6.1E-10	4.5E-09	4.0E-12	2.2E-08	0	0	18.4	81.6	0
R7	14.1	10/12/20	8.1E-08	1.1E-24	8.1E-08	1.7E-08	5.8E-08	1.7E-10	6.0E-09	0	0	92.6	7.4	0
R8	15.3	10/12/20	7.1E-08	4.4E-25	7.1E-08	1.3E-08	5.7E-08	9.4E-11	8.6E-10	0	0	98.8	1.2	0
R10	17.8	10/12/20	7.6E-08	5.7E-22	7.6E-08	1.8E-08	5.5E-08	1.9E-10	2.9E-09	0	0	96.2	3.8	0
R11	24.9	10/12/20	5.8E-08	5.5E-23	5.8E-08	6.8E-09	4.2E-08	3.9E-11	8.4E-09	0	0	85.5	14.5	0
R12	29.5	10/12/20	5.4E-08	1.6E-27	5.4E-08	4.1E-09	4.9E-08	1.4E-11	9.4E-10	0	0	98.3	1.7	0

Supplementary information – Materials and methods

Reagents, materials and solutions

All the solutions were prepared with deionized water (18.2 MΩ cm^{-1} resistivity, Milli-Q water, Millipore). High purity acids were obtained by distillation (Savillex DST-1000 system) from HCl (Merck, Emsure 37 %) and HNO_3 (VWR Chemicals, Normapur 68 %). The following chemicals were used: Na2CO3 (VWR Chemicals, Analar Normapur), Na_2CO_3 (VWR Chemicals, Analar Normapur), $C_8H_5KO_4$ (VWR Chemicals, Analar Normapur), H_3PO_4 (VWR Chemicals, Normapur 85 %), UTEVA resin (100-150 µm mesh, Triskem internationnal). The following standard solutions were used: uranium standard solution (1 g L^{-1}, matrix 2 % HNO_3, CPAChem), multi-element standard solution VIII (24 elements, 100 mg L^{-1}, matrix 6 % HNO_3, Supelco, Certipur), anion chromatography standard solution including Cl^-, Br^-, NO_3^-, NO_2^-, SO_4^{2-} and PO_4^{3-} (100 mg L^{-1}; matrix deionized water, CPAChem).

Chemical analyses

Concentration of anions SO_4^{2-}, NO^{3-}, Cl^-, F^-, Br^- and PO_4^{3-} was measured using ionic chromatography (Metrohm 930 Compact IC) equipped with trap (Metrosep C; 37 – 74 µm particle diameter 4 mm i.d. × 30 mm), guard column (Metrosep A Supp 5; 5 µm particle diameter, 4 mm i.d. × 5 mm) coupled with analytical column (Metrosep A Supp 5; 5 µm particle diameter, 4 mm i.d. × 150 mm), a 250 µL PEEK injection loop, a thermostatic column oven set at 35.0 ± 0.1°C, a mobile phase containing 3.2 mmol L^{-1} Na_2CO_3 and 1 mmol L^{-1} $NaHCO_3$, a MSM suppressor using regenerant solution containing 500 mmol L^{-1} H_3PO_4, and a conductivity detector. The flow rate of mobile phase was fixed at 700 µL min^{-1}. Standard solutions were freshly prepared in deionized water.

Total dissolved carbon (TC) was determined by measuring the CO_2 released after combustion at 850 °C, using a carbon analyzer (Elementar TOC Vario). Dissolved inorganic carbon (DIC) was determined on another aliquot by measuring the amount of CO_2 released after acidification with a 1 M H_3PO_4 solution (final pH < 2). Dissolved organic carbon (DOC) then was calculated by subtracting DIC from TC.

Concentration of the chemical elements Ca, Na, K, Si, Mg, Ba and Sr was determined using ICP-OES (Thermo Fisher Scientific iCAP 7600 Duo). Calibration standards were prepared in 0.3 M HNO_3 in the range of 0.02 – 30 mg L^{-1}.

The determination of U and Se concentrations and ($^{234}U/^{238}U$) activity ratio was performed using Agilent 8800 Inductively coupled plasma-Tandem mass spectrometry ICP-MS/MS (Agilent Technologies, Tokyo, Japan) equipped with an octupole collision/reaction cell (CRC) situated between two mass-selecting analysers. A Peltier-cooled (2 °C) Scott-type spray chamber with a MicroMist nebulizer (*ca.* 400 µL min^{-1}) was employed as introduction system. For Se concentration, ICP-MS/MS analysis was conducted by using the MS/MS with pure oxygen (≥ 99.999 %, Air Products, Aubervilliers, France) as reaction gas (Balcaen, Bolea-fernandez, Resano, & Vanhaecke, 2015; Gronbaek-Thorsen, Stürup, Gammelgaard, & Hyrup Moller, 2019). The oxygen flow rate in CRC was fixed at 3.5 L min^{-1}. Selenium was measured in mass shift mode on *m/z* 94 ($^{78}Se^{16}O^+$). Rhodium as internal standard was added with a T-piece, and its initial signal on *m/z* 103 ($^{103}Rh^+$) was 50,000 – 70,000 cps. Standard Se solutions (up to 10 µg L^{-1}) were prepared in 300 mmol L^{-1} HNO_3. The single MS mode was used to quantify U concentration in sample aliquots, following a measurement protocol already described (Gourgiotis et al., 2020). The activity of U isotopes was calculated from the analytical response of the double isotope reference standard (IRMM 3636) and was corrected from the instrumental mass bias factor using the reference value (Condon, McLean, Noble, & Bowring, 2010; Richter et al., 2008).